

THE ROLE OF SPEG IN *VIBRIO CHOLERAE* BIOFILM FORMATION

A Thesis
by
CAITLIN KIRWIN WOTANIS

Submitted to the Graduate School
at Appalachian State University
in partial fulfillment of the requirements for the degree of
MASTER OF SCIENCE

August 2017
Department of Biology

THE ROLE OF SPEG IN *VIBRIO CHOLERAE* BIOFILM FORMATION

A Thesis
by
CAITLIN KIRWIN WOTANIS
August 2017

APPROVED BY:

Dr. Ece Karatan
Chairperson, Thesis Committee

Dr. Andrew Bellemer
Member, Thesis Committee

Dr. Cara Fiore
Member, Thesis Committee

Dr. Zack Murrell
Chairperson, Department of Biology

Max C. Poole, Ph.D.
Dean, Cratis D. Williams School of Graduate Studies

Copyright by Caitlin Kirwin Wotanis 2017
All Rights Reserved

Abstract

THE ROLE OF SPEG IN *VIBRIO CHOLERAE* BIOFILM FORMATION

Caitlin Kirwin Wotanis
B.A., Appalachian State University
M.S., Appalachian State University

Chairperson: Dr. Ece Karatan

Vibrio cholerae is a Gram-negative, aquatic bacterium responsible for the human disease cholera, which causes watery diarrhea and sometimes death. Human illness typically results from ingestion of the bacterium from its aquatic environment, where it exists mostly as a biofilm. It is known that polyamines– ubiquitous, cationic molecules– regulate biofilm formation. *V. cholerae* is capable of taking up the polyamine norspermidine through the PotABCD1 ABC-type transporter. Additionally, norspermidine can act as an extracellular signal by interaction with the NspS/MbaA signaling complex, whereby norspermidine binding to the NspS periplasmic-binding protein inhibits MbaA phosphodiesterase activity, increasing levels of cyclic diguanylate monophosphate, *Vibrio* polysaccharide gene expression, and biofilm formation. *V. cholerae* is able to synthesize norspermidine through the decarboxylation of carboxynorspermidine by the enzyme NspC, encoded by the *nspC* gene. Interestingly, mutants overexpressing *nspC* from a plasmid have been shown to form 3-5-fold more biofilms than the wild-type strain. However, even under these conditions, internal norspermidine levels do not show any increase. Norspermidine can be toxic to cells

if internal concentrations are too high; therefore, cells could secrete norspermidine into the extracellular environment to mitigate toxicity. However, previous work has found no presence of norspermidine in analyzed culture medium, suggesting that this polyamine is not being secreted as is, and is perhaps being modified. I hypothesized that one strategy to modify norspermidine and avert norspermidine toxicity could involve the enzyme spermidine/spermine-*N'*-acetyltransferase (SpeG), which is encoded by the *speG* gene. SpeG modifies some polyamines by acetylating the primary amine group, giving the molecule an overall neutral charge and facilitating its transport out of the cell. I further hypothesized that an acetylated form of norspermidine could also be sensed by NspS, leading to an inhibition of MbaA, and an increase in biofilm formation. The objective of this study was to elucidate the role of SpeG in *V. cholerae* biofilm formation and determine whether acetylated polyamines act through NspS/MbaA to regulate biofilm formation. To do this, we overexpressed the *speG* gene from a plasmid in various backgrounds and assayed biofilm levels. We found that overexpressing *speG* leads to a significant increase in biofilm formation in a NspS/MbaA-dependent manner. In an effort determine if the signal causing the increase in biofilm formation was internal or external, conditioned media biofilm assays were utilized. When *speG* overexpression media was added to various strains, biofilm formation was significantly increased in a NspS/MbaA-dependent manner. Taken together, our data suggests that a secreted signal from the *speG* overexpression strain is enhancing biofilm formation through the NspS/MbaA signaling complex in *V. cholerae*.

Acknowledgments

I would like to acknowledge the Office of Student Research for its support of this project in the form of monetary grants for both research and travel. This project was also supported in part by NIH grant AI096358 from the National Institute of Allergy and Infectious Diseases awarded to Dr. Ece Karatan. I would like to thank Dr. Andrew Bellemer and Dr. Cara Fiore for not only serving on my Thesis committee, but also for their insightful conversations and guidance. Special thanks go to my advisor, Dr. Ece Karatan, for all of her support, guidance, and encouragement throughout my graduate career. She provided me with an incredibly meaningful education and quality training, while encouraging my self-confidence and self-direction in studying Molecular Biology.

Dedication

I would like to dedicate this work to my family and friends, who have always encouraged me to pursue my dreams and to never give up.

Table of Contents

Abstract.....	iv
Acknowledgments.....	vi
Dedication.....	vii
List of Tables	ix
List of Figures.....	x
Introduction.....	1
Materials and Methods.....	16
Results.....	31
Discussion.....	56
References.....	65
Vita.....	73

List of Tables

Table 1. Bacterial strains.....	17
Table 2. Plasmids	18
Table 3. Primers	18

List of Figures

Figure 1. Structures of the diamines diaminopropane, putrescine, and cadaverine, and the triamines norspermidine and spermidine	3
Figure 2. Model of the polyamine synthesis, transport, and signaling pathways	5
Figure 3. Working model of the NspS-MbaA signaling complex	7
Figure 4. Effect of <i>nspC</i> overexpression on biofilms	8
Figure 5. Effect of <i>nspC</i> overexpression on polyamine composition	8
Figure 6. Schematic diagram of spermidine/spermine N^1 -acetyltransferase enzymatic activity.....	9
Figure 7. Allosteric polyamine-binding site	11
Figure 8. Predicted substrate-binding site.....	13
Figure 9. Construction of the pWM91:: <i>AspeG</i> conjugation plasmid	20
Figure 10. Construction of the pWM91:: <i>AspeG</i> :: <i>tet^R</i> conjugation plasmid	23
Figure 11. Gel electrophoresis of digested pCRSP and pWM91.....	32
Figure 12. Colony PCR depicting successful transformation of pCW1 into <i>E. coli</i> DH5 α pir, which confirms the presence of the <i>AspeG</i> insert in pWM91	32
Figure 13. Colony PCR depicting successful transformation of pCW1 into <i>E. coli</i> SM10 λ pir, which confirms the presence of the <i>AspeG</i> insert in pWM91	33
Figure 14. Confirmation of successful amplification of <i>AspeG</i> :: <i>tet^R</i>	34
Figure 15. Colony PCR depicting successful transformation of pCW2 into <i>E. coli</i> DH5 α , which confirms the presence of the <i>AspeG</i> :: <i>tet^R</i> insert in pCR2.1	34
Figure 16. Gel electrophoresis of digested pCW3 and pWM91	35

Figure 17. Colony PCR depicting successful transformation of pCW3 into <i>E. coli</i> DH5 α pir, which confirms the presence of the <i>AspeG::tet^R</i> insert in pWM91	36
Figure 18. Colony PCR depicting successful transformation of pCW3 into <i>E. coli</i> SM10 λ pir, which confirms the presence of the <i>AspeG::tet^R</i> insert in pWM91	37
Figure 19. Confirmation of successful amplification of <i>speG</i>	37
Figure 20. Colony PCR depicting successful transformation of pCW5 into <i>E. coli</i> DH5 α , which confirms the presence of the the <i>speG</i> insert in pCR2.1	38
Figure 21. Colony PCR depicting successful transformation of pCW6 (<i>pspeG</i>) into <i>E. coli</i> DH5 α , which confirms the presence of the <i>speG</i> insert in pFLAG-CTC	39
Figure 22. Colony PCR depicting successful transformation of pFLAG-CTC and <i>pspeG</i> into <i>V. cholerae</i> wild type (PW357) and <i>ΔnspS</i> (PW514)	40
Figure 23. Colony PCR depicting successful transformation of pFLAG-CTC and <i>pspeG</i> into <i>V. cholerae nspC::kan^R</i> (AK314)	40
Figure 24. Colony PCR depicting successful transformation of <i>pspeG</i> into <i>V. cholerae ΔpotD1</i> (AK160)	41
Figure 25. Colony PCR depicting successful transformation of pFLAG-CTC into <i>V. cholerae ΔpotD1</i> (AK160)	41
Figure 26. Western Blot analysis depicting expression of SpeG protein	42
Figure 27. Model of the polyamine synthesis, transport, acetylation, and signaling pathways	43
Figure 28. Biofilm assay of <i>V. cholerae</i> wild type with <i>pspeG</i> or pFLAG-CTC	44
Figure 29. Biofilm assay of <i>V. cholerae nspC::kan^R</i> with <i>pspeG</i> or pFLAG-CTC	46
Figure 30. Biofilm assay of <i>V. cholerae ΔpotD1</i> with <i>pspeG</i> or pFLAG-CTC	47
Figure 31. Biofilm assay of <i>V. cholerae ΔnspS</i> with <i>pspeG</i> or pFLAG-CTC	48
Figure 32. Effect of <i>pspeG</i> or pFLAG-CTC conditioned medium on wild type, <i>nspC::kan^R</i> , <i>ΔpotD1</i> , and <i>ΔnspS</i> biofilm formation	49
Figure 33. <i>N</i> ⁸ -acetylspermidine and polyamine standard	50
Figure 34. Polyamine content in <i>pspeG</i> culture medium	51

Figure 35. Polyamine content in pFLAG-CTC culture medium	52
Figure 36. Polyamine content in <i>nspC::kan^R</i> , without <i>pspeG</i> , culture medium	53
Figure 37. Cellular polyamine content of wild-type <i>V. cholerae</i> with <i>pspeG</i> and pFLAG-CTC	55
Figure 38. Hypothetical model of the role of SpeG in <i>V. cholerae</i> biofilm formation.....	57

Introduction

Vibrio cholerae is a Gram-negative bacterium that inhabits aquatic ecosystems worldwide and is the intestinal pathogen responsible for the diarrheal disease cholera. In more developed countries, water purification systems have essentially eradicated the risk of exposure to this pathogen; however, in less developed countries water is often obtained directly from rivers or lakes, resulting in an increased risk of exposure to the pathogen [1]. The bacterium exists in two main states: a motile, planktonic stage and a sessile or biofilm stage. In its aquatic habitat this bacterium is thought to exist mostly as a biofilm [2, 3]. The bacterium is ingested by the human host both in its planktonic and biofilm form. It is believed that *V. cholerae* forms biofilms as a survival mechanism, as such structures have been shown to aid in protection against pH and osmotic stress, UV radiation, as well as antimicrobials and the host's immune response [4-7]. It is estimated that approximately 10^4 to 10^6 total cells are required to cause the cholera disease [8]. The accumulation of bacteria within biofilms that may be attached to surfaces, plankton, and aquatic insects is thought to provide a much higher concentration of bacteria than in their planktonic form [9]. Therefore, ingestion of biofilms by the human host is not only believed to confer resistance of *V. cholerae* to the low pH of the stomach [10], but may also provide an adequate number of bacteria to facilitate infection [9]. Additionally, biofilm formation in aquatic reservoirs may allow bacterial persistence between cholera outbreaks [11].

Biofilm formation is a process that includes four distinct stages. Planktonic cells first approach the surface using flagellar motility. Attractive interactions with the surface then facilitate attachment. Changes in gene expression, perhaps due to detection of a favorable environment or an increase in levels of the prokaryotic second messenger cyclic di-guanosine monophosphate, cause these planktonic, motile bacteria to become sessile [12, 13]. These sessile bacteria initiate exopolysaccharide synthesis by expressing *Vibrio* polysaccharide (*vps*) genes, forming the bulk of a matrix which ultimately encapsulates the bacteria along with other molecules such as extracellular DNA, proteins, absorbed nutrients, and metabolites [14, 15]. It is hypothesized that eventually due to changes in gene expression or environmental signals, the biofilm ruptures and the cells disperse into the environment. Once in the aquatic environment, dispersal may allow the free-swimming bacteria to relocate and initiate a new biofilm, potentially becoming the source of a new outbreak [11].

Cells that disperse in the human intestine must first penetrate the intestinal mucosal barrier, after which they adhere, multiply, and form microcolonies on the crypt-villus axis of the small intestine [16]. Cells along the crypt-villus axis begin producing the cholera toxin (CT), an AB₅ family ADP-ribosyltransferase that is responsible for the massive, watery diarrhea characteristic of the cholera disease [17]. The bacterial cells that are excreted along with the stool into the environment can go on to form biofilms elsewhere.

Biofilm formation and maturation, including depth and architecture, appear to be regulated by nutrient availability, quorum sensing, as well as surface composition, osmolarity, and polyamines [18, 19]. Polyamines are flexible aliphatic chains containing two or more amine groups that are positively charged at physiological pH [20]. These natural polycations are involved in cell growth and development of both prokaryotic and eukaryotic

cells [20]. These molecules are found mostly in the form of diamines and triamines, including diaminopropane, putrescine, cadaverine, norspermidine and spermidine (Fig. 1). The diamine putrescine and triamine spermidine are present in virtually all eukaryotic and prokaryotic cells. The diamine cadaverine is synthesized in plants by the decarboxylation of lysine, and is also widespread in Proteobacteria [21]. The polyamine diaminopropane is synthesized by plant polyamine oxidases and is a major polyamine in *Acinetobacter*, *Enterobacter*, and *Vibrionaceae* [21]. The unusual triamine norspermidine has been found in some extremophilic Archaea, in some aquatic and terrestrial plants, and lower aquatic eukaryotes including some diatoms, algae, arthropods, mollusks, and sea squirts [21-25]. Of importance, *V. cholerae* synthesizes putrescine, diaminopropane, cadaverine, and norspermidine.

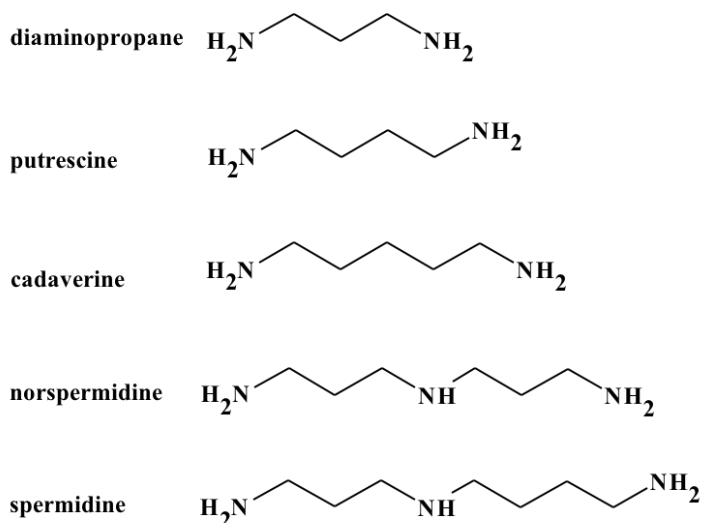


Fig. 1. Structures of the diamines diaminopropane, putrescine, and cadaverine, and the triamines norspermidine and spermidine. Structures were drawn using the ChemSketch program.

While polyamines are believed to perform different functions in different organisms, they have been shown to play a role in biofilm formation in a variety of bacteria, including *V. cholerae* [19, 26]. Although the polyamines norspermidine and spermidine differ in just one

methylene group, they have been shown to influence biofilm formation in *V. cholerae* in opposite ways. Specifically, spermidine inhibits biofilm formation while norspermidine activates biofilm formation [19, 27]. Although spermidine is not typically synthesized by the bacterium [26], it is abundant in the human intestine. It is the dominant polyamine synthesized by the human microbiota [28] and the human diet supplies the body with hundreds of micromoles of spermidine per day [29]. Norspermidine is synthesized by *V. cholerae* through the decarboxylation of carboxynorspermidine by the enzyme NspC, encoded by the *nspC* gene (Fig. 2). Deletion of *nspC* reduces biofilm formation; however, the addition of norspermidine to the growth medium increases biofilms more than 2-fold [26].

Both norspermidine and spermidine are imported into the cell by an ABC-type transporter [27, 30]. The periplasmic substrate-binding protein of the transport system binds polyamines. This leads to the association of the periplasmic-binding protein with the cytoplasmic membrane-bound permease complexes of the transporter. The polyamine is consequently released and transported into the cytoplasm by ATP hydrolysis catalyzed by the ATPase of the transporter [31]. In *V. cholerae*, the norspermidine/ spermidine transporter is composed of PotD1 (the periplasmic substrate-binding protein), PotB and PotC (the two transmembrane permeases), and PotA (the ATPase); (Fig. 2); [27, 30]. All components of the PotABCD1 transport system are believed to be involved in spermidine and norspermidine uptake, although norspermidine appears to be the preferential polyamine substrate for this system (Villa, Sanders, Karatan, unpublished data) [27, 32]. Interestingly, $\Delta potA$, $\Delta potB$, $\Delta potC$, and $\Delta potD1$ mutants all display increased biofilm formation. Additionally, independent deletions of the *potA*, *potB*, *potC*, and *potD1* genes inhibit spermidine uptake, suggesting that the disruption of spermidine import into the cell may mediate this phenotype

[30]. Furthermore, when norspermidine is added to the growth medium of double mutants that both disrupt the synthesis of norspermidine, as well as one of the components of the polyamine transporter, neither norspermidine nor spermidine are detected in the cell.

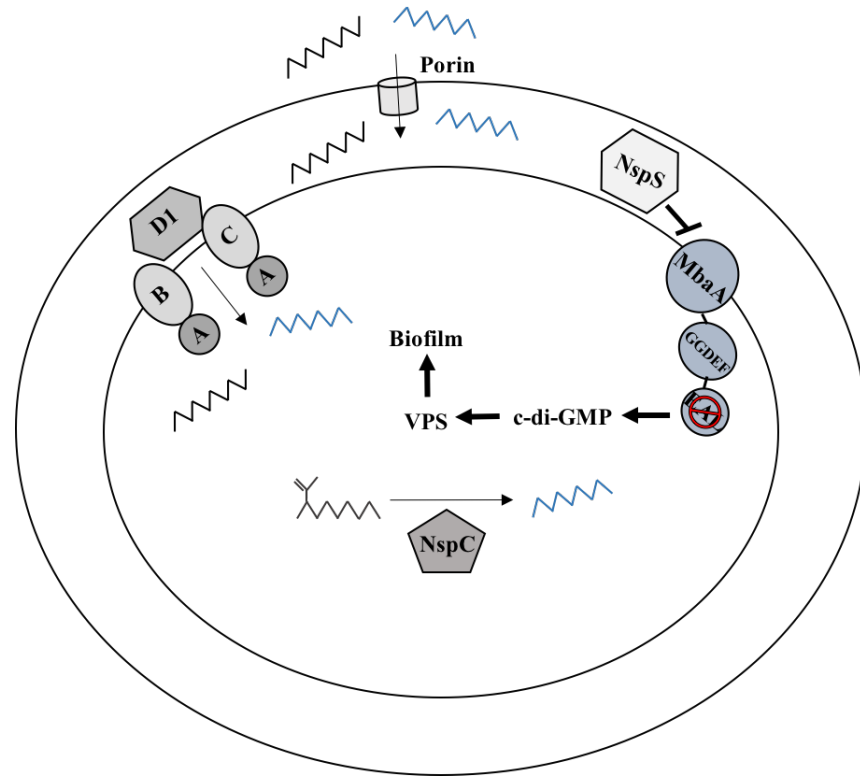


Fig 2. Model of the polyamine synthesis, transport, and signaling pathways. NspC synthesizes norspermidine by the decarboxylation of carboxynorspermidine. Exogenous spermidine and norspermidine may enter the periplasm through a porin where they can be further transported through the PotABCD1 ABC-type transporter or sensed by the NspS/MbaA signaling complex. MbaA contains a GGDEF domain that functions as a diguanylate cyclase and a EAL domain that functions as a phosphodiesterase. Norspermidine bound to NspS inhibits MbaA phosphodiesterase activity, represented by a “no” symbol. Inhibition of phosphodiesterase activity leads to increased levels of c-di-GMP, *Vibrio* polysaccharide (VPS), and biofilm formation. Norspermidine is represented by a blue zig-zag, spermidine is represented by a black zig-zag, and carboxynorspermidine is represented by a branched zig-zag. The PotABCD1 transporter is denoted as A, B, C, and D1.

Norspermidine and spermidine not only act as intracellular signals, but also extracellular signals for regulating biofilm formation [27]. In *V. cholerae* the periplasmic-binding protein NspS is an activator of biofilm formation through binding of polyamines. NspS has been shown to bind norspermidine and spermidine *in vitro* [32]. The *nspS* gene is

cotranscribed with the *mbaA* gene, suggesting that these proteins work together to process polyamine signals [32]. The *mbaA* gene encodes a putative inner membrane-bound protein, MbaA, that is believed to be involved in signal transduction. MbaA contains a GGDEF domain that functions as a diguanylate cyclase, catalyzing the conversion of GTP to c-di-GMP, the bacterial secondary messenger responsible for increased biofilm formation. Increased levels of c-di-GMP activates expression of *vpsT*, and in turn *vpsR*. Both VpsT and VpsR enhance transcription of the *vps* genes and biofilm formation. Conversely, MbaA also contains an EAL domain, which functions as a c-di-GMP phosphodiesterase, degrading c-di-GMP to the linear 5'-phosphoguanylyl-(3',5')-guanosine (pGpG) [19, 32, 33]. Indeed, MbaA has been shown to break down c-di-GMP to pGpG, but not c-di-AMP, suggesting that MbaA is a c-di-GMP-specific phosphodiesterase and repressor of biofilms [32].

In the current model, ligand-free NspS is believed to interact with MbaA and down-regulate its phosphodiesterase activity, leading to intermediate c-di-GMP levels and expression of the *vps* genes [19, 32]. Norspermidine binding to NspS is believed to enhance the inhibitory effect of NspS on MbaA, leading to an increase in biofilm formation. In contrast, binding of spermidine to NspS is believed to inhibit a NspS-MbaA interaction, facilitating maximal MbaA phosphodiesterase activity, decreasing c-di-GMP levels, expression of *vps* genes, and ultimately inhibiting biofilm formation (Fig. 3); [32].

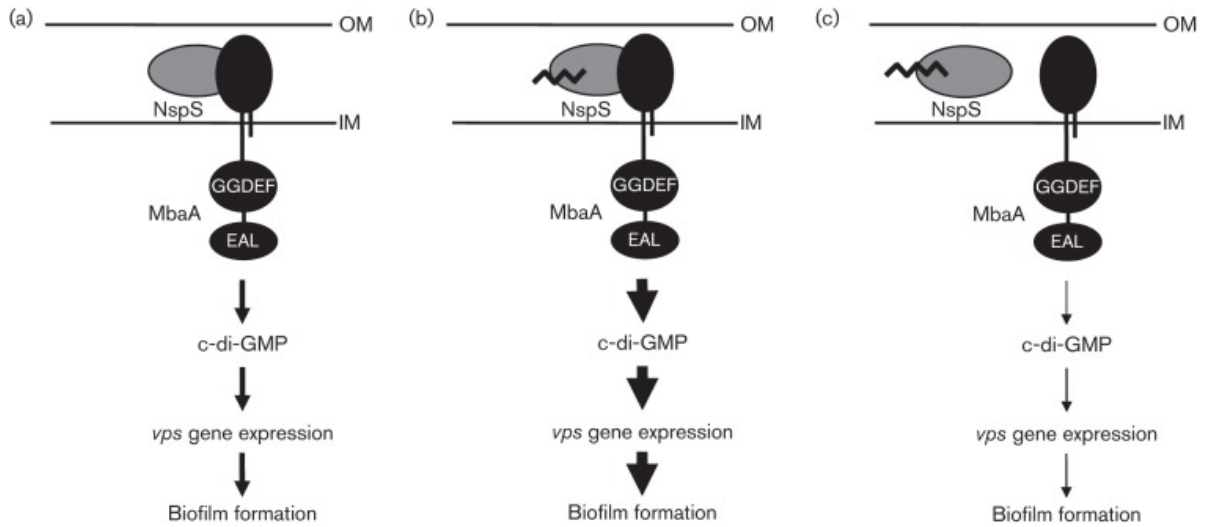


Fig. 3. Working model of the NspS-MbaA signaling complex. Environmental inputs are communicated to the interior of the cell as a change in the enzymatic activity of MbaA. This change is reflected in the c-di-GMP levels, which in turn influence *vps* gene expression and biofilm formation. **(a)** In the absence of a ligand. **(b)** With norspermidine. **(c)** With spermidine. Thin, thicker and thickest arrows correlate with low, medium and high c-di-GMP levels, *vps* gene expression, and biofilm formation. Short and long zig-zag lines bound to NspS represent norspermidine and spermidine, respectively. IM, inner membrane; OM, outer membrane [32].

Interestingly, mutants overexpressing *nspC* from a plasmid have been shown to form 3-5 fold more biofilms than the wild-type strain (Fig. 4); [34]. However, even under these conditions, internal norspermidine levels do not show any increase. Norspermidine can be toxic to cells if internal concentrations are too high; therefore, in response to high concentrations cells could secrete norspermidine into the extracellular environment in an effort to avoid toxicity. However, previous work has found that spent culture medium shows no presence of norspermidine (Fig. 5), suggesting that this polyamine is not being secreted into the culture medium as is [34].

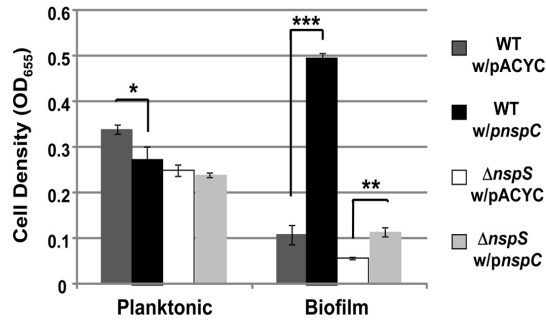


Fig. 4. Effect of *nspC* overexpression on biofilms. Biofilms were formed in borosilicate tubes in LB broth for 18 h. Error bars show standard deviations of six replicates. * $p < 0.05$; ** $p < 0.005$; *** $p < 0.0005$. *pnpC*, *nspC* overexpression strain. Modified from Parker *et al.* 2012 [34].

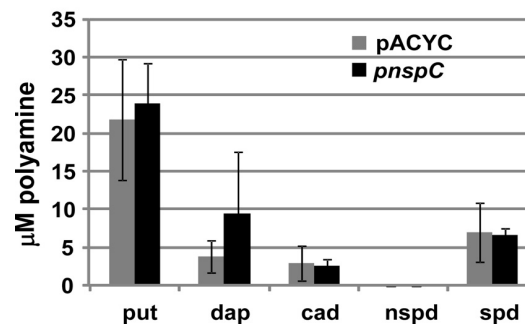


Fig. 5. Effect of *nspC* overexpression on polyamine composition. Polyamines were extracted from conditioned media, derivative by benzoylation, and analyzed by HPLC. Error bars show standard deviations of three biological replicates. Putrescine (put), diaminopropane (dap), cadaverine (cad), norspermidine (nspd), and spermidine (spd). Modified from Parker *et al.* 2012 [34].

Polyamines are not only involved in cell growth and development of both prokaryotic and eukaryotic cells [35, 36], but these polycations also function to stabilize nucleic acids, regulate transcription and translation, as well as control enzymatic activities and modulation of ion channels. Many processes of cells are controlled by polyamines, suggesting that intracellular concentrations of polyamines must be kept within a narrow range. The level of polyamine content is maintained below cellular toxicity and above the requirement for cell growth. Polyamine uptake mechanisms, as well as polyamine biosynthetic pathways

positively regulate intracellular polyamine concentrations, while polyamine export, interconversion, and acetyltransferase enzymes negatively regulate intracellular polyamine levels [37]. While polyamines can be secreted into the extracellular environment to mitigate toxicity, they are often modified by acetylating the primary amine groups prior to secretion [35] using the enzyme spermidine/ spermine-*N*'-acetyltransferase.

The spermidine/ spermine *N*-acetyltransferase enzyme catalyzes the transfer of an acetyl group from acetyl-coenzyme A (acetyl-CoA) to the amine groups of polyamines (Fig. 6). This enzyme plays a significant role in the degradation and interconversion of polyamines, ultimately determining the polyamine concentrations in bacteria and preventing cellular toxicity by the accumulation of these small molecules [38]. The acetylation reaction involves a water molecule that acts as a general base in order to first extract a proton from the terminal primary ammonium ion of the polyamine molecule. The resulting amine group then attacks the carbonyl carbon of the acetyl group from the acetyl-CoA molecule. This reaction forms a tetrahedral intermediate, which is ultimately collapsed once the acetylated product is formed [39].

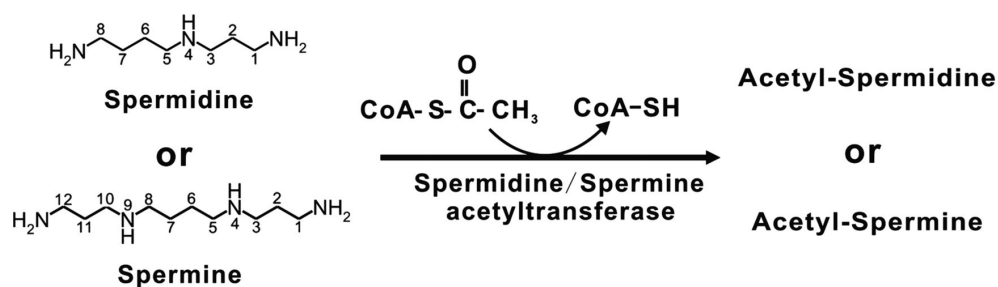


Fig. 6. Schematic diagram of spermidine/spermine *N*¹-acetyltransferase enzymatic activity. Spermidine/spermine *N*¹-acetyltransferase catalyzes the transfer of the acetyl group from acetyl-CoA to spermidine or spermine to produce an acetyl polyamine and free form of CoA. Modified from Zhang, *et al.* 2012 [40].

Polyamine acetyltransferase homologs have been identified and characterized in some bacterial species. These include *V. cholerae* SpeG [38], *Escherichia coli* SpeG [41, 42], *Streptomyces* sp. 139 Ste26 and Ste27 [40, 43], *Bacillus subtilis* BltD and PaiA [39, 44], *Enterococcus faecalis* PmvE [45], and *Staphylococcus aureus* SpeG [46]. In *Escherichia coli*, SpeG has been shown to catalyze the transfer of an acetyl group from acetyl-CoA to the primary amine group of spermidine [38]. Furthermore, when *speG* from a plasmid was introduced into *E. coli* cells, spermidine acetyltransferase activity increased by 8-40 fold [42].

The spermidine *N*-acetyltransferase enzyme in *V. cholerae*, encoded by the *speG* gene, is a 270 kDa species and exists in a dodecameric structure in solution. The SpeG dodecamer is believed to be a dimer of hexamers, where one hexamer is stacked on top of the other. Each monomer within the hexamer forms a dimer with another monomer of the opposite hexamer. Although putrescine and *N*¹-acetylspermine can act as substrates for SpeG, spermine and spermidine are the preferential ligands (specific activity of 3.3, 497, 1400, and 1400 nmol/min/mg, respectively) [47]. The inner surface of the substrate binding pocket of this protein is thought to be negatively charged, suggesting that SpeG prefers to bind positively charged molecules such as polyamines [38].

Spermine and spermidine form specific interactions with the SpeG enzyme to induce acetyltransferase activity. Interestingly, when these ligands were used in co-crystallization trials with SpeG, the binary spermidine- and spermine-liganded structures showed that these two polyamines bind in a pocket outside of the predicted SpeG active site. Additionally, when crystals of SpeG with already bound acetyl-CoA in the active site were soaked with spermine, the structure of SpeG was found to contain CoA in twelve active sites, and spermine bound in an extensive pocket spanning two neighboring monomers outside of the

active site. Considering that the sites containing spermine are located outside of the active site, they were termed the allosteric polyamine-binding sites. Only when the allosteric polyamine-binding site was occupied with spermidine or spermine was there a conformational change of the enzyme as well as specific interactions between the polyamine and the enzyme. Because of their difference in length, spermidine and spermine form distinct hydrogen bonds with the bottom monomer (green) (Fig. 7). Specifically, the N^1 amine of spermidine forms hydrogen bonds with the Glu33 carboxyl, while the N^1 amine of spermine interacts with an oxygen of Glu33. Further, the N^1 amine of spermine (or spermidine) is in close proximity to the acetyl group of acetyl-CoA. Finally, the N^{10} and N^{14} atoms of spermine (or N^{10} of spermidine) may form hydrogen bonds with Glu84 and Glu75. Therefore, the Glu33, Glu84, and Glu75 residues of the binding site are believed to play a significant role in binding and recognizing long polyamines in the binding pocket (Fig. 7). This may explain why shorter polyamines such as putrescine and cadaverine are not able to induce the allosteric loop movement, which is necessary to convert the enzyme to its active form [38].

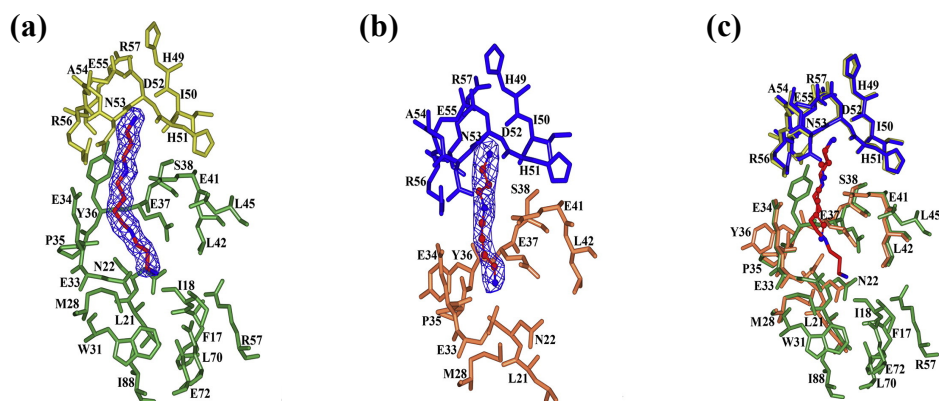


Fig. 7. Allosteric polyamine-binding site. The spermine/spermidine allosteric site is shown: top and bottom monomers for the spermine binding pocket **(a)** are colored yellow and green, respectively; top and bottom subunits for spermidine **(b)** are in blue and orange, respectively. **(c)** Superposition of spermine and spermidine binding pockets. Spermine and spermidine are shown as a stick model and as a ball-and-stick model, respectively, where carbon atoms are in red and nitrogen atoms are in blue. Modified from Filippova EV, *et al.* 2015 [38].

Previous work has suggested that there are two polyamine-binding sites of SpeG that regulate acetyltransferase activity. The first site corresponds to the allosteric polyamine-binding site and has a high affinity for the polyamine ($K_{d1} = 1.6 \mu\text{M}$), while the second site corresponds to the substrate-binding site and has a low affinity ($K_{d2} = 833 \mu\text{M}$). Additionally, it was found that acetyl-CoA binds to SpeG with low affinity ($K_d = 610 \mu\text{M}$) in the absence of spermidine. Therefore, SpeG binds to spermidine with two different affinities and acetyl-CoA binds poorly to SpeG without polyamine bound in the allosteric site [38]. It is believed that SpeG uses a bireactant random steady-state mechanism, whereby the enzyme first binds spermidine or spermine in the allosteric site, which then induces a shift of the allosteric loop to bind acetyl-CoA and an additional polyamine molecule in random order (Fig. 8). It is hypothesized that at low concentrations of spermidine or spermine, the allosteric site is initially filled and converts the enzyme to its active form so it can begin catalysis once high concentrations of the polyamines are reached. Therefore, it has been suggested that SpeG may regulate polyamine acetylation only when intracellular free polyamine concentrations are high, as to not disturb the required polyamine concentration necessary for cellular growth and function [38].

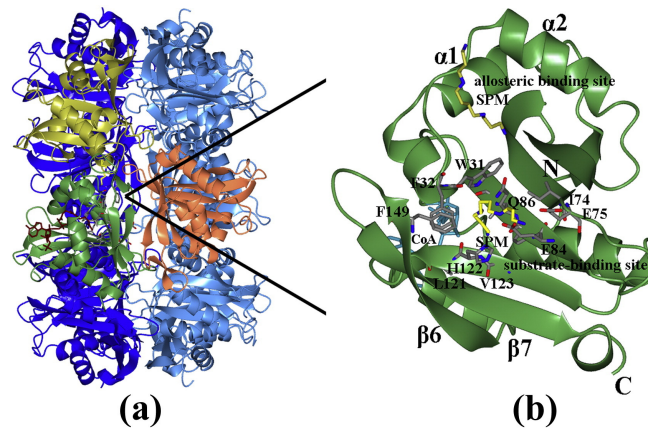


Fig. 8. Predicted substrate-binding site. (a) Ribbon diagram of SpeG dodecamer in complex with CoA (maroon) and spermine (yellow) in the allosteric binding site. Subunits forming the GNAT dimer are colored green and orange. (b) Modeled spermine (yellow) docked into the predicted substrate-binding site of the SpeG structure in complex with CoA (cyan) and spermine (yellow) in allosteric site is shown in one subunit. Secondary structural elements and residues (gray) that make up the substrate-binding site are labeled. The atoms of the residues making up the substrate binding pocket are colored as follows: carbon in gray, oxygen in red, and nitrogen in blue. The atoms of the spermine are colored as follows: carbon in yellow and nitrogen in blue. The N- and C-termini are indicated [38].

Spermidine/spermine N^1 -acetyltransferases, such as *V. cholerae* SpeG, are believed to not only regulate polyamine metabolism, but also to affect the polyamine biosynthetic pathway, ultimately influencing other parts of cell physiology [48]. Because intracellular polyamine concentrations must be kept within a narrow range and finely controlled by enzymes involved in both synthesis and acetylation, spermidine/ spermine N^1 -acetyltransferases may act to maintain polyamine homeostasis within the cell, confer various virulence strategies, as well as serve to regulate the expression of various gene products [39, 45, 46]. Therefore, it is clear that these various acetyltransferase enzymes work to maintain polyamine concentrations within the cell, affecting the bacterium's survival and persistence in its environment.

As previously mentioned, biofilm formation is 3-5-fold higher in a mutant overexpressing *nspC* than wild-type *V. cholerae*. However, intracellular levels of

norspermidine do not increase in this mutant and furthermore, norspermidine is not detected in the spent medium of this mutant, indicating that norspermidine neither accumulates in the cytoplasm, nor is it exported into the extracellular environment [34]. *V. cholerae* SpeG may be one mechanism to avert norspermidine accumulation and toxicity within the cells. Of importance, *V. cholerae* SpeG has also been shown to use norspermidine as a substrate (Misty Kuhn, personal communication). Additionally, the presence of acetyl-norspermidine has been reported in *V. parahaemolyticus* [49]. Therefore, I hypothesized that SpeG acetylates norspermidine to facilitate its transfer out of the cell to mitigate intracellular toxicity. Interestingly, previous work has found that in a NspS-deficient strain, biofilm formation is significantly reduced compared to the *nspC* overexpression strain. Furthermore, in a strain harboring both an overexpressed *nspC* gene and NspS deficiency, biofilm formation is significantly reduced compared to the *nspC* overexpression strain (Fig. 4) [34]. These results suggest that perhaps this acetylated norspermidine is acting through NspS to enhance biofilm formation. Therefore, I further hypothesized that once transported out into the extracellular environment, acetylated norspermidine can bind the periplasmic binding protein NspS, inhibiting MbaA and therefore increasing levels of c-di-GMP, *vps* gene expression, and biofilm formation.

The objective of this study was to elucidate the role of SpeG in *V. cholerae* biofilm formation. I found that overexpressing *speG* leads to a significant increase in biofilm formation in a NspS/MbaA-dependent manner. Furthermore, when conditioned media from a *speG* overexpression strain was added to various *V. cholerae* strains, biofilm formation was significantly increased in a NspS/MbaA-dependent manner. Taken together, my data

suggests that a secreted signal from the *speG* overexpression strain is enhancing biofilm formation through the NspS/MbaA signaling complex in *V. cholerae*.

Materials and Methods

Bacterial strains, plasmids, primers, media, and reagents

The bacterial strains, plasmids, and primers used in this study are listed in Table 1, Table 2, and Table 3, respectively. Primer synthesis for PA238, PA239, PA279, PA280, PA281, PA282, PA297, PA305, and PA306 and DNA sequencing were performed by Eurofins MWG Operon (Huntsville, AL). Primer synthesis for PA315 and PA316 was performed by Sigma-Aldrich (St. Louis, MO). Strains were grown on Luria-Bertani (LB) (1 % tryptone, 0.5 % yeast extract, 85 mM NaCl) agar with relevant antibiotics for 24 hours at 27 °C unless otherwise stated. Antibiotics were added at the following concentrations, unless otherwise stated: for *V. cholerae* 100 µg/ml streptomycin (sm) (FisherBiotech, Fair Lawn, NJ) and ampicillin (amp) (FisherBiotech), 2.5 µg/ml for tetracycline (tet) (FisherBiotech); for *E. coli* 100 µg/ml amp. Cultures were grown in LB broth. The polyamines- putrescine, diaminopropane, cadaverine, norspermidine, and spermidine- were purchased from Sigma-Aldrich (St. Louis, MO).

Table 1. Bacterial strains

Strain	Genotype	Reference/source
<i>E. coli</i>		
DH5 α	F- Φ 80 <i>lacZ</i> Δ M15 Δ (<i>lacZYA-argF</i>) U169 <i>recA1 endA1 hsdR17</i> (rK-, mK+) <i>phoA supE44</i> λ - <i>thi-1 gyrA96 relA1</i>	Invitrogen
DH5 α λ pir	<i>supE44, \Delta lacU169 hsdR17, recA1 endA1 gyrA96 thi-1 relA1, \lambdapir</i>	[50]
SM10 λ pir	<i>thi thr leu tonA lacY supE recA::RP4-2-Tc::Mu\lambda</i> pirR6K; Km ^R	[51]
AK483	DH5 α with pCRSP	Sobe, Karatan, unpublished data
AK491	DH5 α λ pir with pCW1	This study
AK493	SM10 λ pir with pCW1	This study
AK543	DH5 α with pCW2	This study
AK573	DH5 α λ pir with pCW3	This study
AK579	SM10 λ pir with pCW3	This study
<i>V. cholerae</i>		
PW249	MO10, clinical isolate of <i>V. cholerae</i> O139 from India, Sm ^R	[52]
PW357	MO10 <i>lacZ::vpsLp</i> \rightarrow <i>lacZ</i> , Sm ^R	[53]
PW514	PW357 Δ <i>nspS</i> , Sm ^R	[19]
AK160	PW357 Δ <i>potD1</i> , Sm ^R	[27]
AK314	PW357 <i>nspC::kan^R</i> , Kan ^R , Sm ^R	[32]
AK626	PW357 with pCW6	This study
AK632	PW357 with pFLAG-CTC	This study
AK641	AK314 with pCW6	This study
AK644	AK314 with pFLAG-CTC	This study
AK647	PW514 with pCW6	This study
AK650	PW514 with pFLAG-CTC	This study
AK775	AK160 with pCW6	This study
AK777	AK160 with pFLAG-CTC	This study

Table 2. Plasmids

Plasmid	Genotype	Reference/source
pCR2.1-TOPO	Plasmid for TOPO cloning, Ap ^R	Invitrogen
pACYC184	Cloning plasmid, low copy, Tet ^R , Cm ^R	New England Biolabs
pWM91	<i>oriR6k</i> , <i>lacAα</i> , <i>sacB</i> , homologous recombination plasmid, Ap ^R	[54]
pMM13	pACYC184:: <i>nspC</i>	[34]
pFLAG-CTC	Bacterial vector for cytoplasmic expression of C-terminal FLAG fusion proteins	Sigma-Aldrich
pCRSP	pCR2.1:: <i>ΔspeG</i>	Sobe, Karatan, unpublished data
pCW1	pWM91:: <i>ΔspeG</i>	This study
pCW2	pCR2.1:: <i>ΔspeG::tet^R</i>	This study
pCW3	pWM91:: <i>ΔspeG::tet^R</i>	This study
pCW5	pCR2.1:: <i>speG</i>	This study
pCW6	pFLAG-CTC:: <i>speG</i>	This study

Table 3. Primers

Primer	Description	Sequence
Construction of <i>V. cholerae</i> <i>ΔspeG</i>		
PA279	Forward primer for upstream <i>speG</i> fragment	5'-CCAAGTGTATATGAACCTGAAGGG-3'
PA280	Reverse primer for upstream <i>speG</i> fragment	5'-TTACGAGCGGCCGCAGTCGCCGCGT TCTAATGCTCTAAG-3'
PA281	Forward primer for downstream <i>speG</i> fragment	5'-TGCGGCCGCTCGTAAAGCGAGTAAA GACATGGTTAGC-3'
PA282	Reverse primer for downstream <i>speG</i> fragment	5'-TAACGCATTCTCAAAGAGCGCC-3'
Construction of <i>V. cholerae</i> <i>ΔspeG::tet^R</i>		
PA297	Forward primer for <i>tet^R</i> fragment	5'-TGCGGCCGCTCGTAAACGCAGTC AGGCACCGTG-3'
PA305	Forward primer for downstream <i>speG</i> fragment	5'-CGCGGCTCGTGCTAAAGCGAGTAAA GACATGGTTAGC-3'
PA306	Reverse primer for <i>tet^R</i> fragment	5'-TTAGCACGAGCCGCGTCAGGTCGAG GTGGCCCG-3'
Cloning <i>speG</i> into pFLAG-CTC plasmid for overexpression		
PA238	N26- Forward primer for pFLAG-CTC vector	5'-CATCATAACGGTTCTGGCAAATATTC-3'
PA239	C24- Reverse primer for pFLAG-CTC vector	5'-CTGTATCAGGCTGAAAATCTTCTC-3'
PA315	Forward primer for <i>speG</i> gene with NdeI restriction enzyme site	5'-CATATGAACAGTCAGTTAACGCTTAG-3'
PA316	Reverse primer for <i>speG</i> gene with SalI restriction enzyme site	5'-GTCGACCTCGCTTCTATTTAAGTAC-3'

Deletion of the speG gene

To determine the role of SpeG in biofilm formation, a previously generated *speG* deletion construct was used in attempt to delete the *speG* gene using double homologous recombination with sucrose selection. Fragments containing 468 bp upstream and 438 bp downstream of the *speG* gene were amplified by PCR from *V. cholerae* chromosomal DNA using Phusion polymerase (Fig. 9). In order to fuse the two fragments by overlap extension PCR, internal primers were engineered with complementary sequences allowing for the generation of a recombinant molecule, ultimately lacking the gene of interest. Splicing of these fragments produced an in-frame deletion that removed 458 bp of the 522 bp *speG* gene. This linear construct with the internal deletion of the *speG* gene was previously cloned into the pCR2.1-TOPO vector (Invitrogen, Carlsbad, CA). The *speG* insert was excised from the pCRSP plasmid using *XhoI* and *SpeI* enzymes and ligated into the pWM91 plasmid linearized with the same enzymes (Fig. 9) (Table 2).

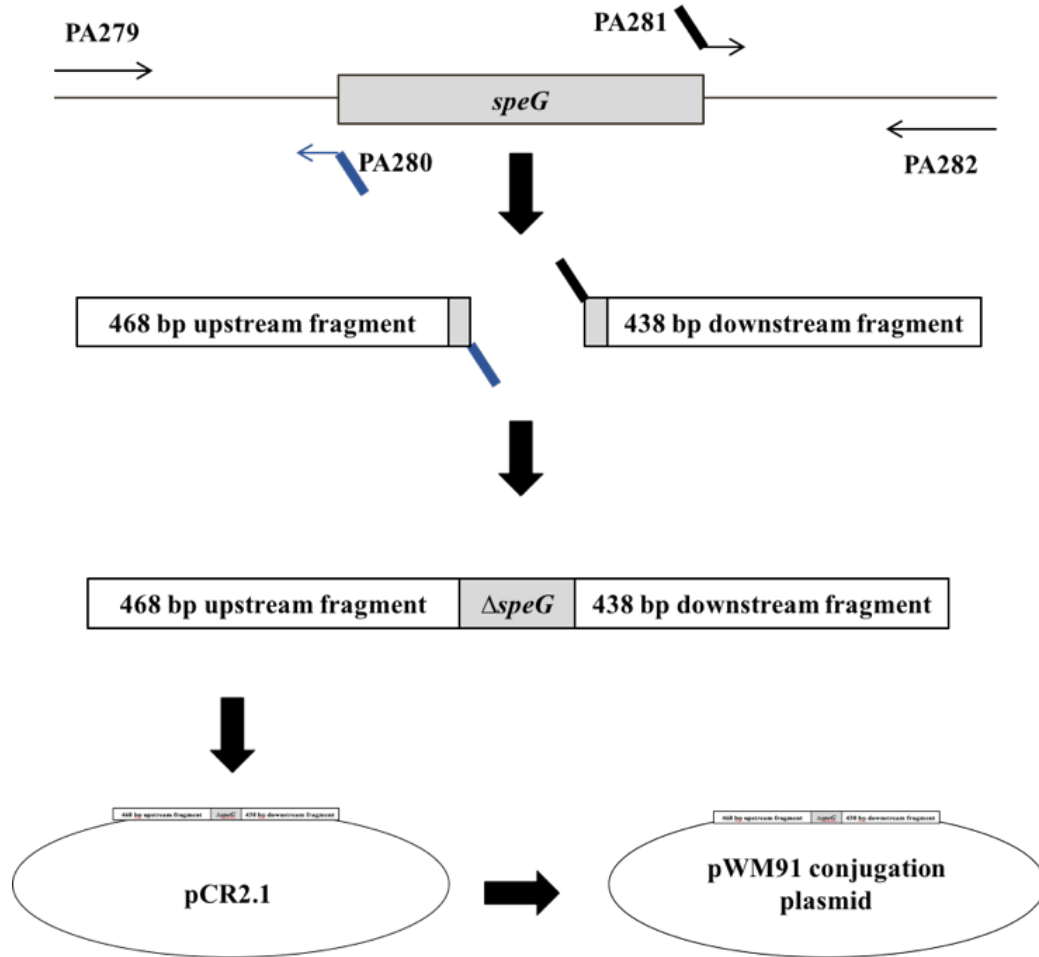


Fig. 9. Construction of the pWM91:: *ΔspeG* conjugation plasmid.

The pCW1 plasmid was then electroporated into electrocompetent *E. coli* DH5 α pir cells using a BIO-RAD MicroPulser (Hercules, CA) at 1.8 kV (Table 2). The transformed cells were recovered by incubation in SOC medium at 37 °C at 200 rpm for 1 hour, and then plated on LB agar plates with 100 μ g/ml amp. Colony PCR was performed to confirm the presence of the *ΔspeG* insert. Single colonies were resuspended in 100 μ l of water and heated at 95 °C for 5 minutes to lyse the cells. Two μ l of this lysate containing template DNA was used in a PCR reaction with 16.4 μ l water, 5 μ l 5X *OneTaq* Standard Reaction Buffer, 0.5 μ l dNTPS, 0.5 μ l of each primer, and 0.125 μ l *OneTaq* DNA polymerase. Cycling conditions

were as follows: initial denaturation at 94 °C for 30 seconds, 35 cycles of 94 °C for 30 seconds, 57.5 °C for 20 seconds, 68 °C for 1 minute, and a final extension at 68 °C for 5 minutes. The PCR products were run on a 1 % agarose gel and colonies positive for the *ΔspeG* insert were grown overnight. This pCW1 plasmid was isolated and then electroporated into electrocompetent *E. coli* SM10λpir cells using a BIO-RAD MicroPulser at 1.8 kV. The transformed cells were recovered as described above. Colony PCR was performed to confirm the presence of the *ΔspeG* insert as described previously.

The *E. coli* SM10λpir strain containing the pCW1 plasmid was used for conjugation with wild-type *V. cholerae* following the SacB counter-selectable mutagenesis protocol, as described by Metcalf *et al.* [54]. Briefly, wild-type *V. cholerae* and donor *E. coli* SM10λpir containing the pCW1 plasmid were streaked on LB plates containing 100 µg/ml sm and 100 µg/ml amp, respectively, and incubated overnight at 27°C and 37°C, respectively. The next day, the *E. coli* SM10λpir with pCW1 strain was mated with the recipient *V. cholerae* wild-type strain on LB plates and incubated overnight at 37°C. After mating, strains were streaked on selection plates containing 100 µg/ml sm and 50 µg/ml amp to select for a single crossover event because *V. cholerae* has a chromosomal streptomycin marker and pCW1 contains an ampicillin resistance marker (Table 1). However, cells were not viable on these selection plates and therefore, the SacB counter-selectable mutagenesis process could not be continued. The possibility remained that in the absence of the *speG* gene, there would be an accumulation of norspermidine or spermidine at levels toxic to the cells. Therefore, The *E. coli* SM10λpir strain containing the pCW1 plasmid was also used for conjugation with various *V. cholerae* norspermidine and/or spermidine-null mutants, including *nspC::kan^R*,

ΔpotDI, and *nspC::kan^RΔpotDI* mutants following the SacB counter-selectable mutagenesis protocol. However, cells were not viable on the selection plates after mating.

Next, a tetracycline resistance cassette was utilized to interrupt the *speG* gene, while also serving as a positive selection marker. Fragments containing 468 bp upstream and 432 bp downstream of the *speG* gene were amplified by PCR from *V. cholerae* chromosomal DNA using Phusion polymerase (Fig. 10). Additionally, a tetracycline resistance cassette was amplified from the pACYC184 plasmid. The primers were designed such that PA280, the reverse primer used for amplification of the upstream fragment of *speG*, contained complementary regions to PA297, the forward primer used for amplification of the *tet^R* gene. Likewise, PA305, the forward primer used for the amplification of the downstream fragment of *speG*, contained complementary regions to PA306, the reverse primer for amplification of the *tet^R* gene. These three PCR products were spliced together by overlap extension PCR (Fig. 10).

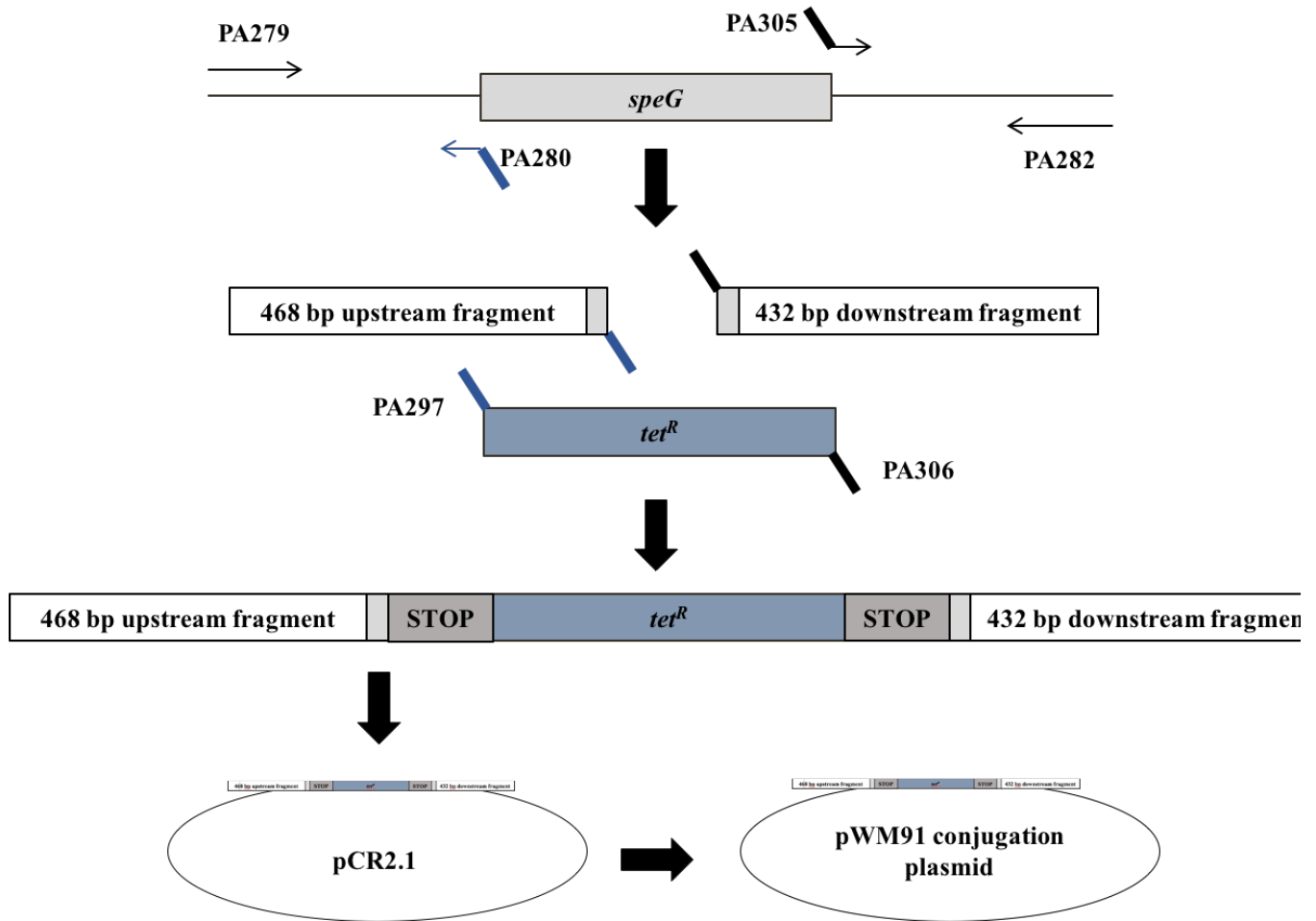


Fig. 10. Construction of the pWM91::*ΔspeG*::*tet^R* conjugation plasmid.

After purification of the *ΔspeG*::*tet^R* PCR product, adenines were added to the 3' ends of the blunt ended fragments for TA cloning. Following manufacturer's instructions, 10 μ l of PCR product was mixed with 33.5 μ l water, 5 μ l *OneTaq* polymerase buffer, 1 μ l dATP (10 mM), and 5 μ l *OneTaq* polymerase and incubated at 72 $^{\circ}$ C for 10 minutes. This PCR product with adenines was then cloned into a linearized pCR2.1-TOPO vector with single thymine overhangs following manufacturer's instructions (Invitrogen, Carlsbad, CA) and electroporated into electrocompetent *E. coli* DH5 α using a BIO-RAD MicroPulser (Hercules, CA) at 1.8 kV (Fig. 9). The transformed cells were recovered by incubation in SOC medium

at 37 °C at 200 rpm for 1 hour, and then plated on LB agar plates with 100 µg/ml amp and 20 µg/ml X-Gal (in dimethyl sulfoxide).

Blue-white screening was used to select for plasmids carrying the *ΔspeG::tet^R* insert and colony PCR using primers PA279 and PA282 was performed to confirm the presence of the insert, as described previously (Table 3). Cycling conditions were as follows: initial denaturation at 94 °C for 30 seconds, 35 cycles of 94 °C for 30 seconds, 62 °C for 15 seconds, 68 °C for 1.5 minutes, and a final extension at 68 °C for 5 minutes. The PCR products were run on a 0.8 % agarose gel and colonies positive for the *ΔspeG::tet^R* insert were grown overnight. The next day, the pCW2 plasmid, with *ΔspeG::tet^R* cloned into pCR2.1, was purified using the Promega Wizard Plus SV Miniprep DNA Purification System (Madison, WI) and sent out for sequencing.

The sequence of the insert were verified by services provided by Eurofins MWG Operon (Huntsville, AL). The *ΔspeG::tet^R* insert was excised using XhoI and SpeI, and ligated into the pWM91 plasmid linearized with the same enzymes (Fig. 9). This pCW3 plasmid was then electroporated into electrocompetent *E. coli* DH5αλpir cells using a BIO-RAD MicroPulser (Hercules, CA) and verified using colony PCR, as described previously. Next, this plasmid was isolated and then electroporated into electrocompetent *E. coli* SM10λpir cells using a BIO-RAD MicroPulser and verified using colony PCR, as described previously. The *E. coli* SM10λpir strain containing the pWM91::*ΔspeG::tet^R* plasmid was used for conjugation with wild-type *V. cholerae* following the SacB counter-selectable mutagenesis protocol as described by Metcalf *et al.* [54]. Briefly, the recipient wild-type *V. cholerae* and donor *E. coli* SM10λpir containing the plasmid pWM91::*ΔspeG::tet^R* were streaked on LB plates containing 100 µg/ml sm and 100 µg/ml amp, respectively, and

incubated overnight at 27°C and 37°C, respectively. The next day, the SM10λpir *E. coli* pWM91::*ΔspeG::tet^R* strain was mated with the recipient *V. cholerae* wild type strain on LB plates and incubated overnight at 37°C. After mating, strains were streaked on selection plates containing 100 µg/ml sm, 50 µg/ml amp, and 2.5 µg/ml tet to select for single crossover events. However, cells were not viable on the selection plates and the SacB counter-selectable mutagenesis process could not be continued. The *E. coli* SM10λpir strain containing the pWM91::*ΔspeG::tet^R* plasmid was also used for conjugation with *V. cholerae* *nspC::kan^R* and *ΔpotD1* mutants following the SacB counter-selectable mutagenesis protocol; however, cells were not viable on the selection plates after mating.

Overexpression of the speG gene

Considering attempts to delete the *speG* gene were unsuccessful, the *speG* gene was instead overexpressed from a plasmid to assess the role of SpeG in *V. cholerae* biofilm formation. The *speG* gene was amplified by PCR from *V. cholerae* chromosomal DNA using Phusion polymerase with primers PA315 and PA316 with engineered *NdeI* and *Sall* restriction enzyme sites, respectively (Table 3). After purification of the PCR product, adenines were added to the 3' ends of the blunt ended fragments for TA cloning. Following manufacturer's instructions, 10 µl of PCR product was mixed with 33.5 µl water, 5 µl *OneTaq* polymerase buffer, 1 µl dATP (10 mM), and 5 µl *OneTaq* polymerase and incubated at 72 °C for 10 minutes. This PCR product with adenines was then cloned into a linearized pCR2.1-TOPO vector (Invitrogen, Carlsbad, CA), as described previously, and electroporated into electrocompetent *E. coli* DH5α using a BIO-RAD MicroPulser (Hercules, CA) at 1.8 kV. The transformed cells were recovered by incubation in SOC medium at 37 °C

at 200 rpm for 1 hour, and then plated on LB agar plates with 100 µg/ml amp and 20 µg/ml X-Gal (in dimethyl sulfoxide).

Blue-white screening was used to select for plasmids carrying the *speG* insert and colony PCR was performed, as described previously, to confirm the presence of the insert using primers PA315 and PA316 (Table 3). Cycling conditions were as follows: initial denaturation at 94 °C for 30 seconds, 30 cycles of 94 °C for 30 seconds, 55 °C for 15 seconds, 68 °C for 30 seconds, and a final extension at 72 °C for 5 minutes. The PCR products were run on a 1 % agarose gel and colonies positive for the *speG* insert were grown overnight. The next day, the plasmids were purified using the Promega Wizard Plus SV Miniprep DNA Purification System (Madison, WI) and sent out for sequencing.

Sequences were verified by services provided by Eurofins MWG Operon (Huntsville, AL). The *speG* insert was excised using *NdeI* and *Sall* enzymes and purified using the GE Healthcare Illustra GFX PCR DNA and Gel Band Purification Kit (Buckinghamshire, UK). The inserts were then ligated into the pFLAG-CTC plasmid linearized with the same enzymes using ElectroLigase following manufacturer's instructions (New England BioLabs, Inc. Ipswich, MA) and electroporated into electrocompetent *E. coli* DH5α using a BIO-RAD MicroPulser at 1.8 kV. The transformed cells were recovered by incubation in SOC medium at 37 °C at 200 rpm for 1 hour, and then plated on LB agar plates with 100 µg/ml amp. The next day, colony PCR was performed to confirm the presence of the *speG* insert as described above. Colonies positive for the *speG* insert were grown overnight and the next day, the plasmid was purified using the Promega Wizard Plus SV Miniprep DNA Purification System (Madison, WI). The pCW6 plasmid and empty pFLAG-CTC vector were then electroporated

into electrocompetent *V. cholerae* wild type, *nspC::kan^R*, *ΔnspS*, and *ΔpotDI* mutants using a BIO-RAD MicroPulser at 1.8 kV.

Western Blotting to confirm the presence of the SpeG protein

A single colony of the strains containing the pCW6 plasmid, as well as the strains containing the pFLAG-CTC vector, was used to inoculate a 2 ml LB culture with 100 µg/ml amp. The cultures were grown at 27 °C for 16-18 hours. The next day, cells were pelleted, resuspended in 300 µl 1X phosphate-buffered saline (PBS), and sonicated 3 times for 10 seconds each. The samples were centrifuged at 4 °C for 20 minutes at 16,000 x g. The supernatant was removed and diluted 1:1 with 1X Laemmli sample buffer containing β-Mercaptoethanol and placed in a hot water bath at 65 °C for 5 minutes. Seventeen µl of sample were then loaded on a polyacrylamide denaturing gel with 12 % acrylamide resolving gel and 5 % stacking gel and run at 250 V for 1 hour. The gel and blotting paper were equilibrated in 1X Transfer Buffer containing 50 mM TRIS, 40 mM Glycine, 1.5 mM SDS, and 20 % methanol. A PVDF membrane was briefly immersed in 100 % methanol and then incubated in 1X Transfer Buffer for 15 minutes. The gel was transferred to the membrane using a BIO-RAD Mini Trans-Blot (Hercules, CA) for 25 minutes at 100 V. The membrane was then blocked for 4 hours with 5 % skim milk in 1X PBS with 0.05 % Tween 20 at 4 °C. Next, the membrane was incubated with 3 % skim milk in 1X PBS with 0.05 % Tween 20, an anti-FLAG antibody conjugated to horseradish peroxidase (AbD Serotec, Raleigh, NC), and a Precision Protein™ StrepTactin-HRP Conjugate antibody (BIO-RAD, Hercules, CA) both diluted 1:10,000 for 1 hour at room temperature. After incubating, the membrane was washed three times for 15 minutes in 1X PBS with 0.05 % Tween 20. Next, the membrane

was incubated with SuperSignal West Pico Chemiluminescent Substrate (ThermoScientific, Rockford, IL) for 5 minutes, then imaged using a BIO-RAD Molecular Imager Gel Doc XR System (Hercules, CA).

Biofilm assays

Biofilm assays were performed as previously described [19] in triplicate and repeated at least three times to ensure reproducibility. A single colony was used to inoculate a 2 ml LB culture with appropriate antibiotics added. The culture was grown at 27 °C for 16-18 hours. The next day, the culture was diluted 1:50 in 2 ml fresh LB broth, grown to mid-log phase and used to inoculate 300 µl LB to an OD of 0.02. The cultures were incubated in borosilicate test tubes statically at 27 °C for 24 hours to facilitate biofilm formation. The next day, 150 µl of planktonic cells were removed and placed into a 96-well microplate for optical density reading. The remaining planktonic cells were discarded. The biofilm was washed with 300 µl 1X phosphate-buffered saline (PBS). The biofilm was homogenized by vortexing with 1.0 mm glass beads (BioSpec, Bartlesville, OK) in 300 µl 1X PBS. Then, 150 µl of the homogenized biofilm-PBS mixture was removed and placed into a 96-well microplate. The planktonic and biofilm cell densities were measured using a BIO-RAD iMark MicroPlate Reader (Hercules, CA) at a wavelength of 655 nm.

Conditioned media biofilm assays

A single colony was used to inoculate a 2 ml LB culture with appropriate antibiotics added. The culture was grown at 27 °C for 16-18 hours. The next day, the culture was diluted 1:50 in 2 ml fresh LB broth and grown to mid-log phase. At mid-log phase, cells were

pelleted via centrifugation at 10,000 x g for 5 minutes and the media supernatant was filter-sterilized using a 0.2 µm cellulose acetate membrane (GE Healthcare Bio-Sciences, Pittsburgh, PA). Conditioned media were mixed with fresh LB at a ratio of 2:1 and inoculated with mid-log phase cells to a starting OD₆₅₅ of 0.02 and grown at 27 °C for 24 hours without agitation to allow biofilm formation. After 24 hours, biofilm and planktonic cell density were measured as described above.

Extraction, benzylation, and detection of extracellular polyamines

In order to identify polyamine content in the culture medium, a single colony was used to inoculate a 2 ml LB culture with appropriate antibiotics added. The culture was grown at 27 °C for 16-18 hours. The next day, the culture was diluted 1:20 in 20 ml fresh LB broth with appropriate antibiotics added. Every two hours from 0-6 hours, 1 ml of the culture was removed and pelleted at 10,000 x g for 5 minutes. The supernatant was removed and treated with 50 % (w/v) trichloroacetic acid to precipitate out any potential larger molecules, and centrifuged, leaving the supernatant with polyamines. This supernatant was removed and benzylated as described previously [27]. Briefly, samples were extracted twice with chloroform, evaporated to dryness and dissolved in 100 µl of 60% methanol in water. A standard mix containing 0.1 mM of each polyamine was also prepared and benzylated each time. The set of benzylated polyamine samples were separated using high-performance liquid chromatography (HPLC) with a Phenomenex Spherclone ODS column (5 µm, 250 x 4.6 mm) that was fitted with a 4.0 x 3.0 mm guard cartridge with the system described above. The runs were performed using a gradient of 45-60 % methanol in water for 30 minutes with a 10-minute isocratic equilibration of 45 % methanol in water.

Extraction, benzoylation, and detection of cellular polyamines

In order to identify intracellular polyamine content, polyamines were extracted and analyzed as previously described [27, 34, 55]. Briefly, bacteria were grown at 27 °C to mid-exponential phase, pelleted, washed twice with 1x PBS, and resuspended in 10 µl water per milligram wet cell weight. The cell suspension was lysed using sonication and the cell debris was removed by centrifugation. Cellular proteins were precipitated with 50 % (w/v) trichloroacetic acid and centrifuged, leaving the supernatant with polyamines. This supernatant was removed and benzoylated as described above.

Statistical analyses

Data were analyzed using Student's *t*-test (two-tailed, unpaired). A minimum of three biological replicates were performed for all experiments (unless otherwise noted). Differences were considered statistically significant for *p*-values of 0.05 and below.

Results

Construction of the Δ speG mutant

Norspermidine has been shown to enhance biofilm formation in *V. cholerae* [19]; however, polyamine concentrations must be tightly regulated in cells to avoid toxicity [35]. Spermidine/spermine-*N'*-acetyltransferase (SpeG) in *E. coli* has been shown to catalyze the transfer of an acetyl group from acetyl-CoA to the primary amine group of spermidine, facilitating its transfer out of the cell in an effort to mitigate toxicity [42, 48]. Of importance, a collaborator has shown that SpeG from *V. cholerae* is capable of acetylating norspermidine (Misty Kuhn, personal correspondence). Based on these observations, I hypothesized that in order to avoid intracellular norspermidine toxicity, SpeG catalyzes the transfer of an acetyl group from acetyl-CoA to the primary amine group of norspermidine to facilitate its transfer out of the cell. I further hypothesized that this modified form of norspermidine could be sensed by the periplasmic-binding protein NspS, and ultimately lead to an increase in biofilm formation. To test this hypothesis, I first attempted to construct a Δ speG mutant to assess biofilm formation. The previously constructed plasmid, pCRSP (with Δ speG cloned into the pCR2.1 vector), and the pWM91 plasmid were subjected to a double digest with *XhoI* and *SpeI* enzymes. Lanes 1 and 2 represent the cut pCR2.1-TOPO vector at 3.9 kb containing the Δ speG insert at 865 bp. Lanes 4 and 5 represent the cut pWM91 conjugation plasmid at 8.2 kb (Fig. 11). After gel purifying, the Δ speG gene product was then ligated into the pWM91 vector, forming the pCW1 plasmid, and transformed into *E. coli* DH5 α pir via

electroporation. Thirteen colonies were subjected to a colony PCR to verify they had successfully incorporated the pCW1 plasmid. Lanes 12 and 13 have a band at 865 bp, indicative of the *ΔspeG* insert (Fig. 12).

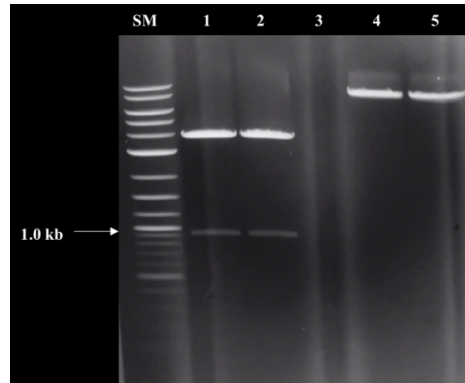


Fig. 11. Gel electrophoresis of digested pCRSP and pWM91. In order to ligate the *ΔspeG* insert into pWM91, pCRSP and pWM91 were digested with XhoI and SpeI and run on a 1 % agarose gel. SM (size marker): NEB 2-log DNA ladder, lanes 1 and 2 contain the cut pCR2.1 plasmid containing the *ΔspeG* insert, and lanes 4 and 5 contain the cut pWM91 plasmid.

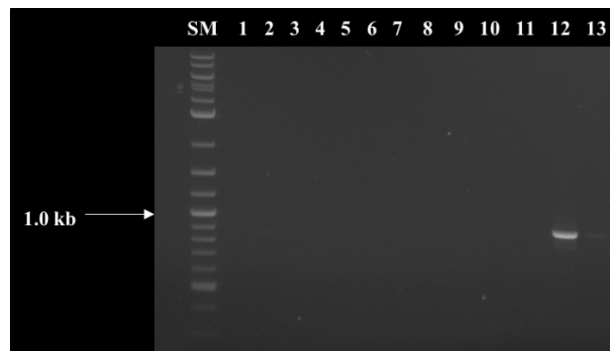


Fig. 12. Colony PCR depicting successful transformation of pCW1 into *E. coli* DH5αλpir, which confirms the presence of the *ΔspeG* insert in pWM91. Thirteen ampicillin-resistant colonies were screened using colony PCR. Primers PA279 and PA282 were used to verify the presence of the *ΔspeG* insert. SM (size marker): NEB 2-log DNA ladder; lanes 1-13: colonies 1-13.

The pCW1 plasmid was extracted and purified from *E. coli* DH5αλpir and transformed into *E. coli* SM10λpir via electroporation. Colonies that grew on ampicillin plates were screened using colony PCR. Lanes 1-6, 8-11, and 13-17 exhibit a band at 865 bp,

indicative of the *ΔspeG* fragment, verifying successful incorporation of the pCW1 plasmid into *E. coli* SM10λpir (Fig. 13). This strain was then used for conjugation into wild-type *V. cholerae* following the SacB counter-selectable mutagenesis protocol, as described by Metcalf *et al.* [54], to construct a *V. cholerae ΔspeG* mutant. However, the cells were not viable when streaked on selection plates, suggesting that the *speG* gene may be essential.

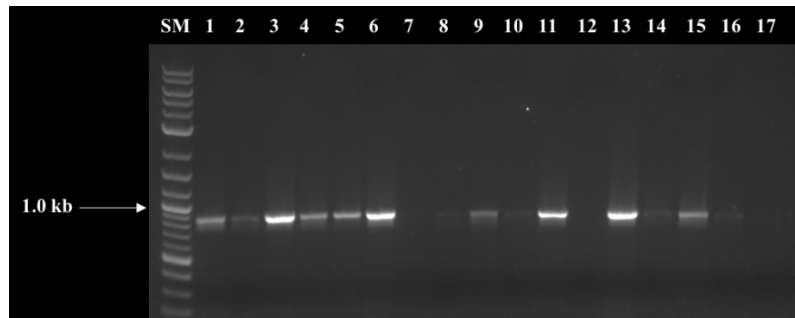


Fig. 13. Colony PCR depicting successful transformation of pCW1 into *E. coli* SM10λpir, which confirms the presence of the *ΔspeG* insert in pWM91. Seventeen ampicillin-resistant colonies were screened using colony PCR. Primers PA279 and PA282 were used to verify the presence of the *ΔspeG* insert. SM (size marker): NEB 2-log DNA ladder; lane 1-17: colonies 1-17.

Construction of the *ΔspeG::tet^R* mutant

Next, a different approach was taken to delete the *speG* gene. The *speG* gene was interrupted with a tetracycline resistance cassette, which could also be used as a positive selection marker. First, a linear construct missing the *speG* gene and containing a tetracycline resistance cassette (*tet^R*) was constructed, as described in Materials and Methods. An upstream fragment of *speG*, a downstream fragment of *speG*, and *tet^R* were all spliced together by overlap extension PCR, as described in Materials and Methods. The PA279 and PA282 primers were used to amplify the *ΔspeG::tet^R* fragment. A band present in lane 1 at 2089 bp is indicative of successful amplification of the *ΔspeG::tet^R* fragment (Fig. 14). This

$\Delta speG::tet^R$ gene product was used for TA cloning, as described in Materials and Methods. The pCW2 plasmid, with $\Delta speG::tet^R$ cloned into the pCR2.1 vector was then transformed via electroporation into *E. coli* DH5 α . Nineteen candidates were subjected to a colony PCR to verify that they had successfully incorporated the pCW2 plasmid. Lanes 4 and 5 have a band present at 2089 bp, indicative of the $\Delta speG::tet^R$ fragment (Fig. 15).

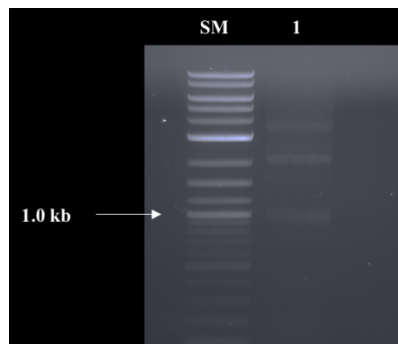


Fig. 14. Confirmation of successful amplification of $\Delta speG::tet^R$. The upstream and downstream regions of the *speG* gene were amplified from chromosomal DNA and the *tet^R* gene was amplified from the pACYC184 plasmid. These products were spliced together by overlap extension PCR. This $\Delta speG::tet^R$ fragment was reamplified in a PCR reaction using primers PA279 and PA282. SM (size marker): NEB 2-log DNA ladder; lane 1 contains the $\Delta speG::tet^R$ gene product at 2089 bp.

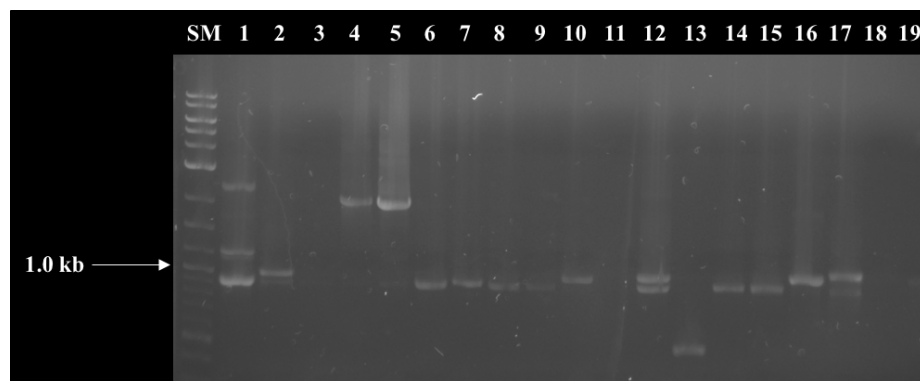


Fig. 15. Colony PCR depicting successful transformation of pCW2 into *E. coli* DH5 α , which confirms the presence of the $\Delta speG::tet^R$ insert in pCR2.1. Nineteen ampicillin-resistant colonies were screened using colony PCR. Primers PA279 and PA282 were used to verify the presence of the $\Delta speG::tet^R$ insert. SM (size marker): NEB 2-log DNA ladder; lane 1-19: colonies 1-19.

Once the sequence of the $\Delta speG::tet^R$ fragment was verified, the pCW2 and pWM91 plasmids were subjected to a double digest with *XhoI* and *SpeI* enzymes (Fig. 16). Lanes 2 and 3 represent the cut pWM91 conjugation plasmid at 8.2 kb. Lanes 5 and 6 represent the cut pCR2.1-TOPO vector at 3.9 kb containing the $\Delta speG::tet^R$ insert at 2089 bp (Fig. 16). After gel purifying, the $\Delta speG::tet^R$ gene product was then ligated into the pWM91 vector, forming the pCW3 plasmid, and transformed into *E. coli* DH5 α pir via electroporation. Nine colonies were subjected to a colony PCR to verify they had successfully incorporated the pCW3 plasmid. Lanes 1, 3-5, and 8-9 have a band at 2089 bp, indicative of the $\Delta speG::tet^R$ insert (Fig. 17).

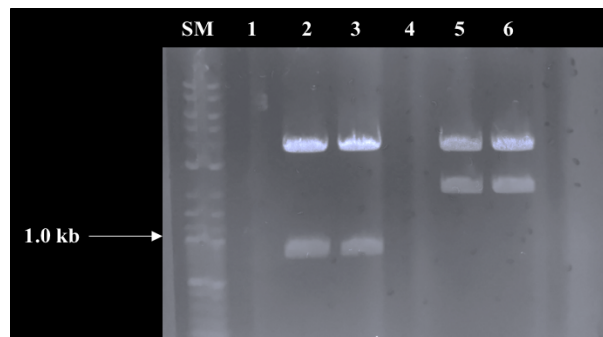


Fig. 16. Gel electrophoresis of digested pCW3 and pWM91. In order to ligate the $\Delta speG::tet^R$ insert into pWM91, pCW3 and pWM91 were digested with *XhoI* and *SpeI* and run on a 0.8 % agarose gel. SM (size marker): NEB 2-log DNA ladder, lanes 2 and 3 contain the cut pWM91 plasmid, and lanes 5 and 6 contain the cut pCR2.1 plasmid containing the $\Delta speG::tet^R$ insert.

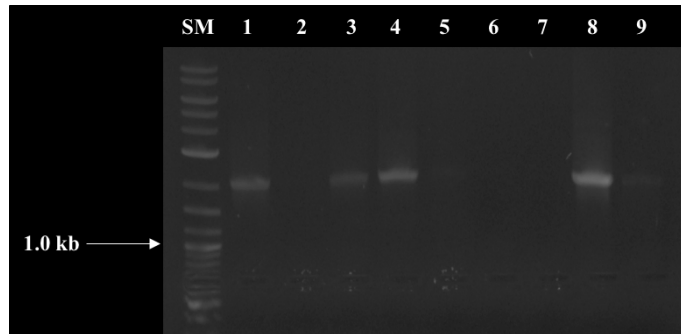


Fig. 17. Colony PCR depicting successful transformation of pCW3 into *E. coli* DH5 α pir, which confirms the presence of the $\Delta speG::tet^R$ insert in pWM91. Nine ampicillin-resistant colonies were screened using colony PCR. Primers PA279 and PA282 were used to verify the presence of the $\Delta speG::tet^R$ insert. SM (size marker): NEB 2-log DNA ladder; lane 1-9: colonies 1-9.

The pCW3 plasmid was extracted and purified from *E. coli* DH5 α pir and transformed into *E. coli* SM10 λ pir via electroporation. Colonies that grew on ampicillin plates were screened using colony PCR. Lanes 1-9 exhibit a band at 2089 bp, indicative of the $\Delta speG::tet^R$ fragment, and verifying successful incorporation of the pCW3 plasmid into *E. coli* SM10 λ pir (Fig. 18). This strain was then used for conjugation into wild-type *V. cholerae* following the SacB counter-selectable mutagenesis protocol, as described by Metcalf *et al.* [54], to construct a *V. cholerae* $\Delta speG::tet^R$ mutant. However, cells were not viable when streaked on selection plates, corroborating previous results suggesting the *speG* gene may be essential.

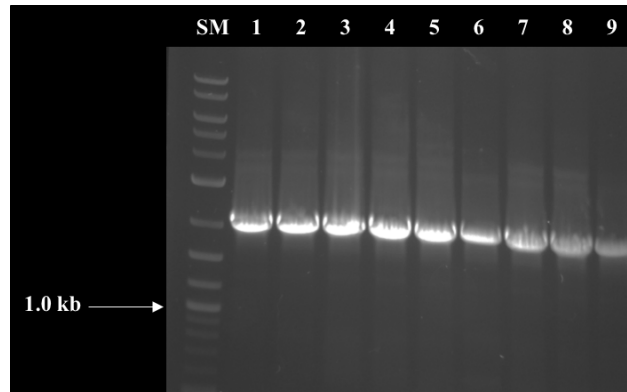


Fig. 18. Colony PCR depicting successful transformation of pCW3 into *E. coli* SM10λpir, which confirms the presence of the $\Delta speG::tet^R$ insert in pWM91. Nine ampicillin-resistant colonies were screened using colony PCR. Primers PA279 and PA282 were used to verify the presence of the $\Delta speG::tet^R$ insert. SM (size marker): NEB 2-log DNA ladder; lane 1-9: colonies 1-9.

Verification of speG overexpression

Considering my attempts to delete the *speG* gene were unsuccessful, I instead overexpressed the *speG* gene from a plasmid in various *V. cholerae* backgrounds to assess the effect of polyamine acetylation on biofilm formation. The *speG* primers were designed to amplify the 522 bp *speG* fragment, with engineered *NdeI* and *Sall* restriction enzymes sites. A band present in lane 1 at 522 bp is indicative of successful amplification of the *speG* gene (Fig. 19).

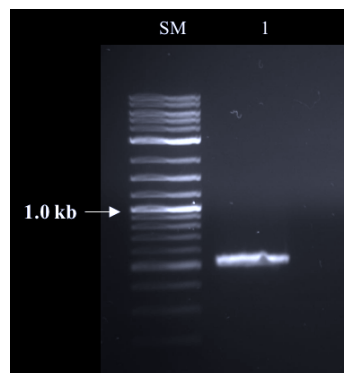


Fig. 19. Confirmation of successful amplification of *speG*. The *speG* gene was amplified in a PCR reaction using primers PA315 and PA316. SM (size marker): NEB 2-log DNA ladder; lane 1 contains the *speG* gene product at 522 bp.

This *speG* product was used for TA cloning, as described previously. The pCW5 plasmid, with *speG* cloned into the pCR2.1 cloning vector, was then transformed via electroporation into *E. coli* DH5 α . Three candidates were subjected to a colony PCR to verify that they had successfully incorporated the pCW5 plasmid. Lanes 1-3 have a band present at 522 bp, indicative of the *speG* fragment (Fig. 20)

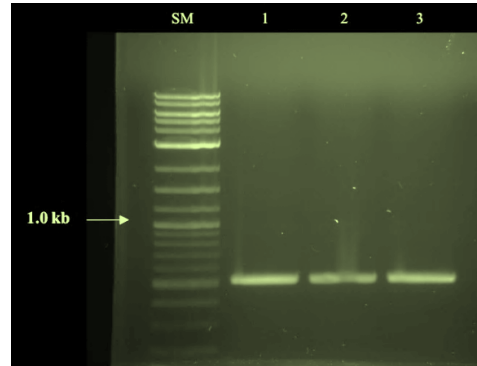


Fig. 20. Colony PCR depicting successful transformation of pCW5 into *E. coli* DH5 α , which confirms the presence of the the *speG* insert in pCR2.1. Three ampicillin-sensitive colonies were screened using colony PCR. Primers PA315 and PA316 were used to verify the presence of the *speG* insert. SM (size marker): NEB 2-log DNA ladder; lane 1-3: colonies 1-3.

Once the sequence of the *speG* gene was verified, the pCW5 and pFLAG-CTC expression vector were each subjected to a double digest with *NdeI* and *Sall* enzymes. After gel purifying, the *speG* gene product was then ligated into the pFLAG-CTC expression vector, forming the pCW6 plasmid, and transformed into *E. coli* DH5 α via electroporation. Nine colonies were subjected to a colony PCR to verify they had successfully incorporated the pCW6 (*pspeG*) plasmid. Lanes 1-9 have a band at 522 bp, indicative of the *speG* insert (Fig. 21).

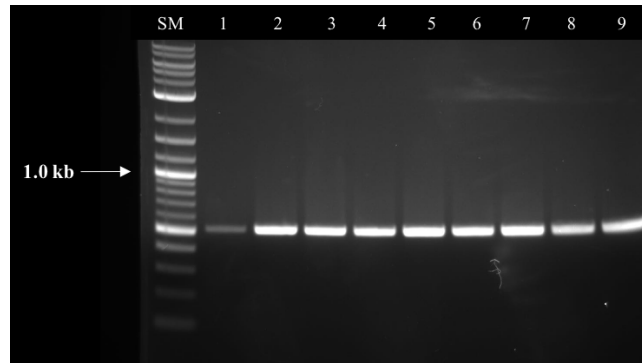


Fig. 21. Colony PCR depicting successful transformation of pCW6 (*pspeG*) into *E. coli* DH5 α , which confirms the presence of the *speG* insert in pFLAG-CTC. Nine ampicillin-resistant colonies were screened using colony PCR. Primers PA315 and PA316 were used to verify the presence of the *speG* insert. SM (size marker): NEB 2-log DNA ladder; lane 1-9: colonies 1-9.

The *pspeG* plasmid was extracted and purified from *E. coli* DH5 α and transformed into *V. cholerae* wild type, *nspC::kan^R*, $\Delta nspS$, and $\Delta potD1$ backgrounds via electroporation. An empty pFLAG-CTC expression vector was also transformed into these same backgrounds via electroporation to be used as a control. Colonies that grew on ampicillin plates were screened using colony PCR. In Fig. 22, lanes 1-4 exhibit a band at 522 bp, indicative of the *speG* fragment, while lanes 5-8 exhibit a band at 222 bp, indicative of the multiple cloning site (MCS) of the empty pFLAG-CTC vector, and confirms successful transformation of *pspeG* and pFLAG-CTC, respectively, into wild-type *V. cholerae*. Lanes 9-12 exhibit a band at 522 bp, indicative of the *speG* fragment, while lanes 13-16 exhibit a band at 222 bp, indicative of the MCS of the pFLAG-CTC vector, and confirms successful transformation of *pspeG* and pFLAG-CTC, respectively, into *V. cholerae* $\Delta nspS$. In Fig. 23, lanes 1-9 exhibit a band at 522 bp, indicative of the *speG* fragment, while lanes 10-18 exhibit a band at 222 bp, indicative of the MCS of the pFLAG-CTC vector, and confirms successful transformation of *pspeG* and pFLAG-CTC, respectively, into *V. cholerae* *nspC::kan^R* mutants. In Fig. 24,

Lanes 1-7 exhibit a band at 744 bp, indicative of the *speG* fragment, verifying successful incorporation of the *pspeG* plasmid into *V. cholerae* Δ *potD1* mutants. In Fig. 25, lanes 1-7 exhibit a band at 222 bp, representing the MCS of the pFLAG-CTC vector, and confirming successful transformation of this plasmid into *V. cholerae* Δ *potD1* mutants.

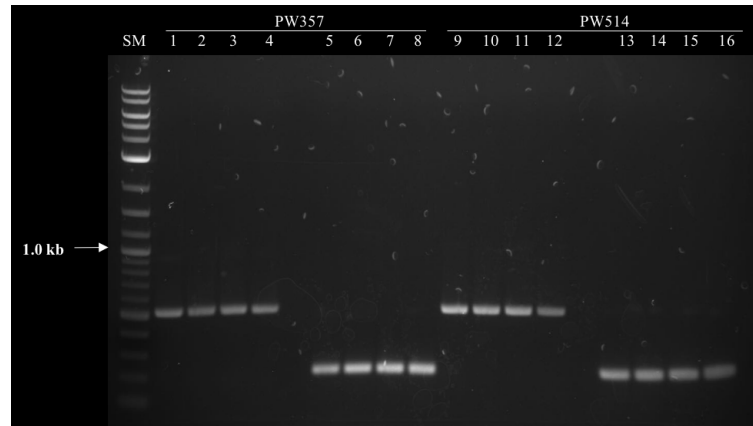


Fig. 22. Colony PCR depicting successful transformation of pFLAG-CTC and *pspeG* into *V. cholerae* wild type (PW357) and Δ *nspS* (PW514). Four ampicillin-resistant colonies were screened using colony PCR. Primers PA238 and PA239 were used to verify the MCS of the pFLAG-CTC empty vector. Primers PA315 and PA316 were used to verify the presence of the *speG* insert. SM (size marker): NEB 2-log DNA ladder; lanes 1-4 represent wild type with *pspeG* colonies; lanes 5-8 represent wild type with pFLAG-CTC colonies; lanes 9-12 represent Δ *nspS* with *pspeG* colonies; lanes 13-16 represent Δ *nspS* with pFLAG-CTC colonies.

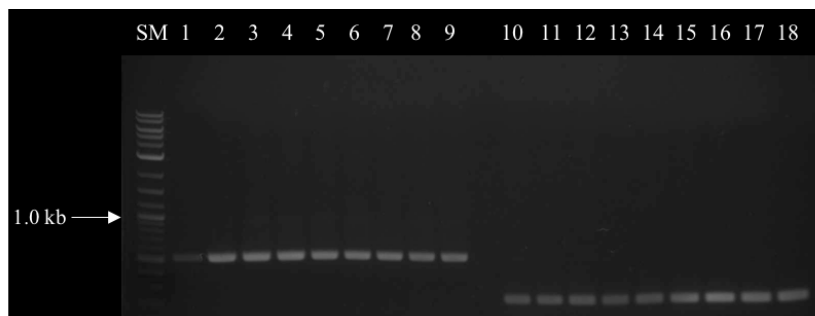


Fig. 23. Colony PCR depicting successful transformation of pFLAG-CTC and *pspeG* into *V. cholerae* *nspC::kan^R* (AK314). Nine ampicillin-resistant colonies were screened using colony PCR. Primers PA238 and PA239 were used to verify the MCS of pFLAG-CTC empty vector. Primers PA315 and PA316 were used to verify the presence of the *speG* insert. SM (size marker): NEB 2-log DNA ladder; lanes 1-9 represent *nspC::kan^R* with *pspeG* colonies; lanes 10-18 represent *nspC::kan^R* with pFLAG-CTC colonies.

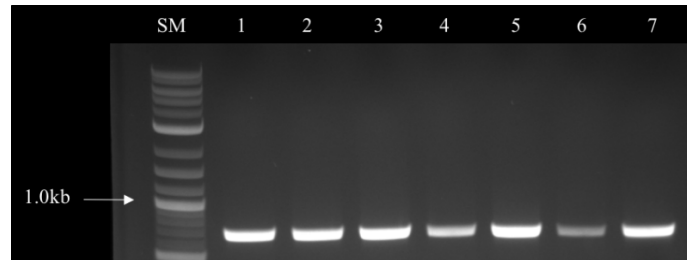


Fig. 24. Colony PCR depicting successful transformation of *pspeG* into *V. cholerae* $\Delta potD1$ (AK160). Seven ampicillin-resistant colonies were screened using colony PCR. Primers PA238 and PA239 were used to verify the presence of the *speG* insert. SM (size marker): NEB 2-log DNA ladder; lanes 1-7 represent $\Delta potD1$ with *pspeG*.

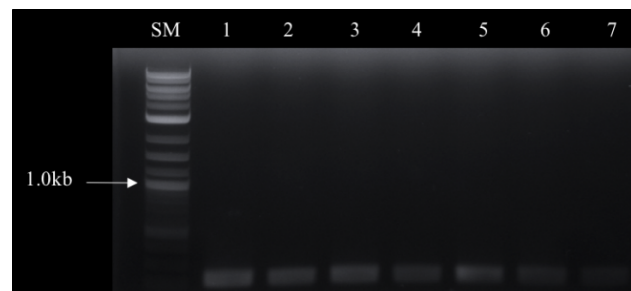


Fig. 25. Colony PCR depicting successful transformation of pFLAG-CTC into *V. cholerae* $\Delta potD1$ (AK160). Seven ampicillin-resistant colonies were screened using colony PCR. Primers PA238 and PA239 were used to verify the MCS of pFLAG-CTC empty vector. SM (size marker): NEB 2-log DNA ladder; lanes 1-7 represent $\Delta potD1$ with pFLAG-CTC colonies.

After confirming that the *pspeG* and pFLAG-CTC plasmids had been successfully transformed into the various *V. cholerae* backgrounds, a Western Blot was performed to confirm the presence of the SpeG protein in each background. The pFLAG-CTC vector was used for cytoplasmic expression of the C-terminal FLAG-tagged SpeG protein and an Anti-FLAG antibody was used to detect the SpeG protein. Around 22.5 kDa, the SpeG protein can be visualized in lanes 1, 3, 5, and 7, corresponding to wild type, *nspC::kan^R*, $\Delta nspS$, and $\Delta potD1$ backgrounds, respectively (Fig. 26). This verified that the wild-type, *nspC::kan^R*, $\Delta nspS$, and $\Delta potD1$ backgrounds, which carry the plasmid with the entire *speG* gene, express the FLAG-tagged SpeG protein.

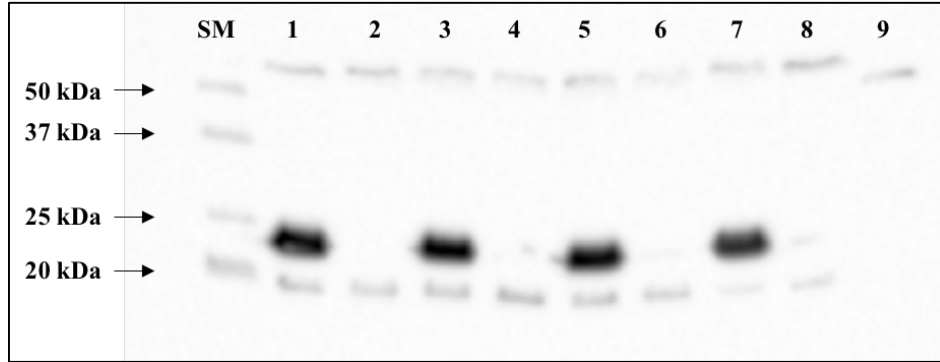


Fig. 26. Western Blot analysis depicting expression of SpeG protein. Cell lysates were separated by SDS-PAGE, blotted, and reacted with anti-FLAG antibody and Precision Protein™ StrepTactin-HRP Conjugate antibody. SpeG was detected using the FLAG-tag. SM (size marker): BIO-RAD Precision Plus Protein™ Dual Color Standard; Lane 1: wild-type *V. cholerae* with *pspeG*; Lane 2: wild-type *V. cholerae* with pFLAG-CTC; Lane 3: *nspC::kan^R* with *pspeG*; Lane 4: *nspC::kan^R* with pFLAG-CTC; Lane 5: $\Delta nspS$ with *pspeG*; Lane 6: $\Delta nspS$ with pFLAG-CTC; Lane 7: $\Delta potD1$ with *pspeG*; Lane 8: $\Delta potD1$ with pFLAG-CTC; Lane 9: positive control of pFLAG-CTS-BAP around 50 kDa. Size of SpeG protein is 22.5 kDa.

Overexpression of speG enhances V. cholerae wild type biofilm formation

Considering a *speG* deletion mutant could not be generated, I overexpressed the *speG* gene from a plasmid to gain insight into the role of SpeG and acetylated polyamines in *V. cholerae* biofilm formation. In wild-type *V. cholerae* norspermidine and spermidine are both sensed by the NspS/MbaA signaling complex and imported into the cell by the PotABCD1 transporter. Norspermidine and spermidine are presumably acetylated by SpeG and their acetylnorspermidine and acetylspermidine products may be transported out of the cell and sensed by NspS to influence biofilm formation (Fig. 27).

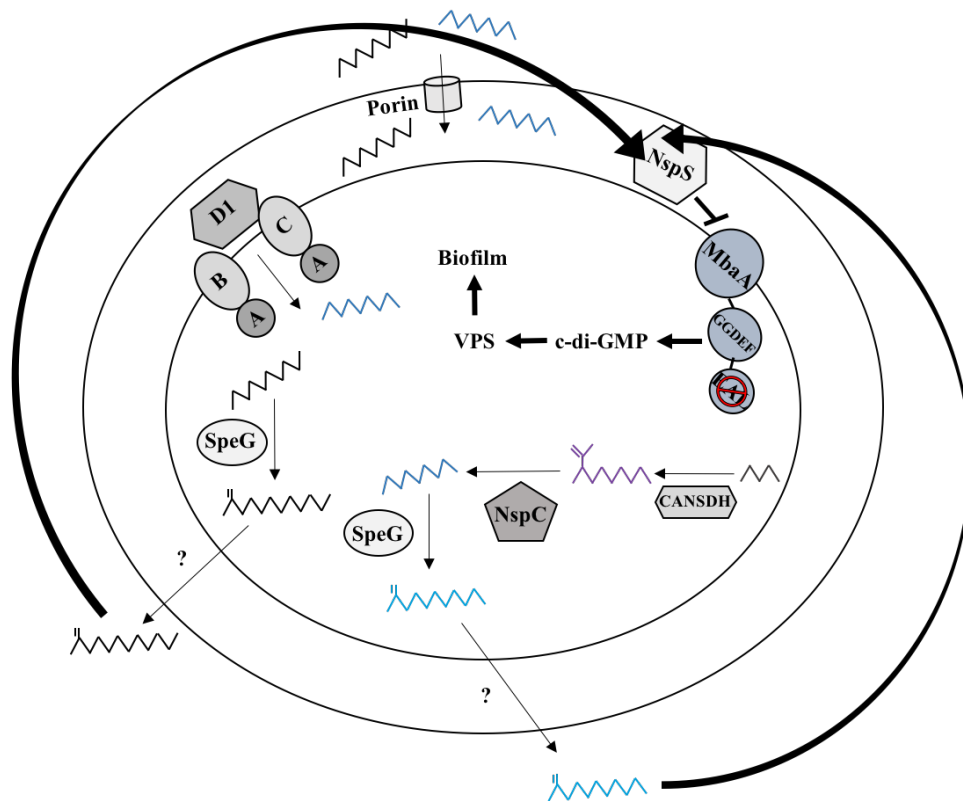


Fig. 27. Model of the polyamine synthesis, transport, acetylation, and signaling pathways. Diaminopropane is converted to carboxynorspermidine by the CANSDH enzyme. Carboxynorspermidine is further converted to norspermidine by NspC. Both spermidine and norspermidine are imported into the cell by the PotABCD1 transporter and sensed by the NspS/MbaA signaling complex. Intracellular spermidine and norspermidine are acetylated by SpeG and exported out of the cell. Acetylated norspermidine bound to NspS may inhibit MbaA phosphodiesterase activity, represented by the “no” symbol. Inhibition of phosphodiesterase activity increases c-di-GMP, *Vibrio* polysaccharide (VPS), and biofilm formation. Acetylated spermidine may also bind to NspS and influence biofilm formation. Diaminopropane is represented by small black zig-zag, carboxynorspermidine is represented by a purple branched zig-zag, norspermidine is represented by a blue zig-zag, spermidine is represented by a black zig-zag, acetyl-norspermidine is represented by a cyan branched zig-zag, and acetyl-spermidine is represented by a black branched zig-zag. The PotABCD1 transporter is denoted as A, B, C, and D1.

To assess the effects of SpeG and polyamine acetylation on biofilm formation, a quantitative biofilm assay was performed on *V. cholerae* wild type that carries the *pspeG* plasmid. Of importance, when ampicillin was added to the cultures, biofilm formation of wild type with *pspeG* varied within each strain. Four replicates exhibited an increase, 9

replicates exhibited a decrease, and 9 replicates exhibited no difference in biofilm formation, when compared to wild type with pFLAG-CTC. Overall, biofilm formation of both strains was significantly lower when grown in the presence of ampicillin, compared to conditions with no ampicillin added. I hypothesized that the addition of the antibiotic may be responsible for these inconsistencies. Ampicillin is a β -lactam antibiotic, and recently, other β -lactam antibiotics were found to be effective for inhibiting biofilms in *Pseudomonas aeruginosa* [56]. Therefore, biofilm assays were conducted without the addition of ampicillin. I found that overexpressing *speG* led to a small, but significant, increase in biofilm formation in wild-type *V. cholerae* (Fig. 28). I hypothesized that this increase in biofilm formation was due to increased acetylnorspermidine being transported out of the cell and consequently sensed by NspS.

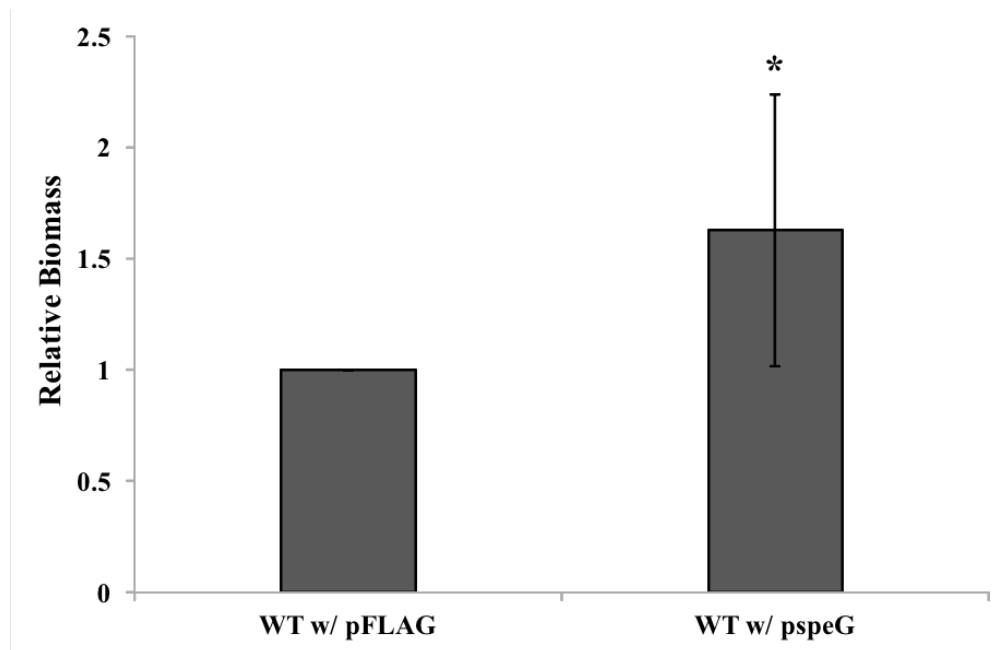


Fig. 28. Biofilm assay of *V. cholerae* wild type with *pspeG* or pFLAG-CTC. Biofilms were formed in borosilicate tubes in LB broth for 24 hours at 27 °C without ampicillin, and quantified as described in Materials and Methods. Relative biomass was calculated using the following equation OD_{655} mutant/ OD_{655} wild-type (Y-axis). Error bars show standard deviations of eight biological replicates. A star indicates a significant difference. A p-value of <0.05 was considered significant. WT, wild type.

Overexpression of speG enhances biofilm formation in a nspC::kan^R mutant

To further test my hypothesis that acetylnorspermidine was being transported out of the cell and consequently sensed by NspS, I next overexpressed the *speG* gene in a *nspC::kan^R* mutant, which does not synthesize norspermidine. Surprisingly, *pspeG* significantly enhanced biofilm formation even in the *nspC::kan^R* background (Fig. 29). This is intriguing considering that because the *nspC::kan^R* mutant is incapable of synthesizing norspermidine, the SpeG protein would be unable to acetylate this polyamine, and the NspS periplasmic-binding protein would therefore be unable to bind this modified polyamine to enhance biofilm formation, as hypothesized. However, it is possible that SpeG enhances biofilm formation in the *nspC::kan^R* mutant by some other mechanism, such as acetylation of another polyamine, like diaminopropane or putrescine, that in its modified form is able to bind NspS and enhance biofilm formation.

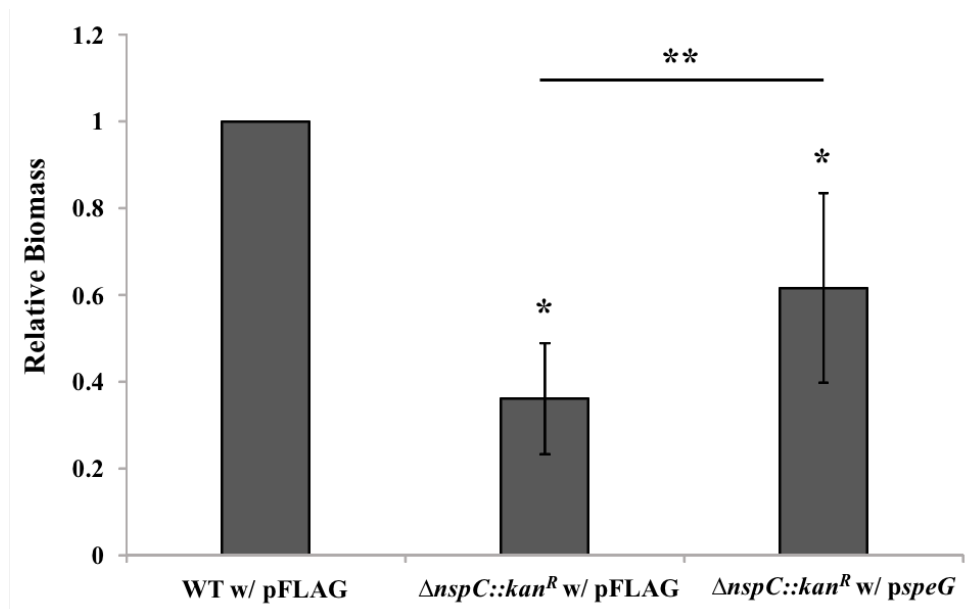


Fig. 29. Biofilm assay of *V. cholerae nspC::kan^R* with *pspeG* or pFLAG-CTC. Biofilms were formed in borosilicate tubes in LB broth for 24 hours at 27 °C without ampicillin, and quantified as described in Materials and Methods. Relative biomass was calculated using the following equation OD_{655} mutant/ OD_{655} wild-type (Y-axis). Error bars show standard deviations of eight biological replicates. A star indicates a significant difference between wild type and the mutants. A double star indicates a significant difference between *nspC::kan^R* with *pspeG* and *nspC::kan^R* with pFLAG-CTC. A p-value of <0.05 was considered significant. WT, wild type.

Overexpression of *speG* in a $\Delta potD1$ mutant has no effect on biofilm formation

As previously mentioned, the PotABCD1 transporter imports both norspermidine and spermidine into the cell. Presumably, SpeG acetylates both intracellular norspermidine and spermidine. Therefore, in a $\Delta potD1$ mutant spermidine would not be imported and SpeG would therefore only acetylate norspermidine. Thus, there would be an accumulation of only acetylnorspermidine in the extracellular environment that could consequently be sensed by NspS. If this is the case, I hypothesized that overexpressing *speG* in a $\Delta potD1$ background would lead to an increase in acetylnorspermidine, and a potential increase in biofilm formation through the NspS/MbaA signaling complex. However, there was no difference in biofilm formation between the $\Delta potD1$ with *pspeG* and $\Delta potD1$ with pFLAG-CTC mutants

(Fig. 30). It is possible that biofilm levels are already at a maximum in this mutant, and so a significant enhancement in biofilm formation by *pspeG* cannot be measured.

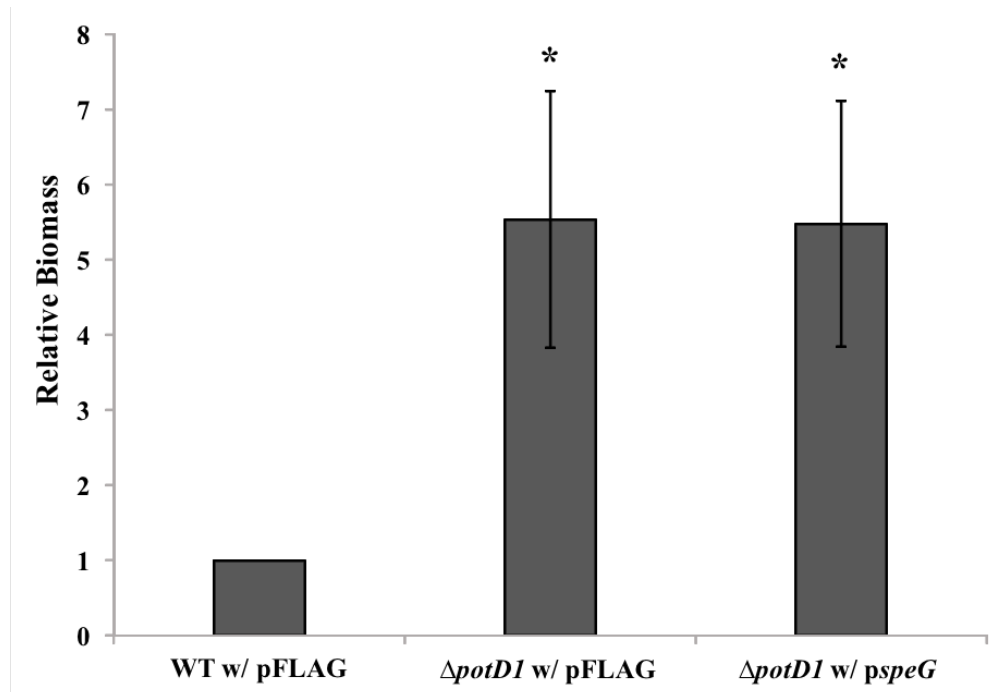


Fig. 30. Biofilm assay of *V. cholerae* $\Delta potD1$ with *pspeG* or pFLAG-CTC. Biofilms were formed in borosilicate tubes in LB broth for 24 hours at 27 °C without ampicillin, and quantified as described in Materials and Methods. Relative biomass was calculated using the following equation OD_{655} mutant/ OD_{655} wild-type (Y-axis). Error bars show standard deviations of eight biological replicates. A star indicates a significant difference between wild type and the mutants. A p-value of <0.05 was considered significant. WT, wild type.

Overexpression of *speG* enhances biofilm formation through *NspS/MbaA*

To further elucidate the mechanism by which *SpeG* enhances biofilm formation in wild type and *nspC::kan^R* mutants, *speG* was overexpressed in a $\Delta nspS$ mutant. Biofilm formation by the $\Delta nspS$ with *pspeG* and $\Delta nspS$ with pFLAG mutants was significantly lower than wild type. Furthermore, there was no difference in biofilm levels between the $\Delta nspS$ with *pspeG* and $\Delta nspS$ with pFLAG-CTC mutants (Fig. 31), consistent with my hypothesis that the metabolite responsible for the increase in biofilm formation acts through the *NspS/MbaA* signal transduction system.

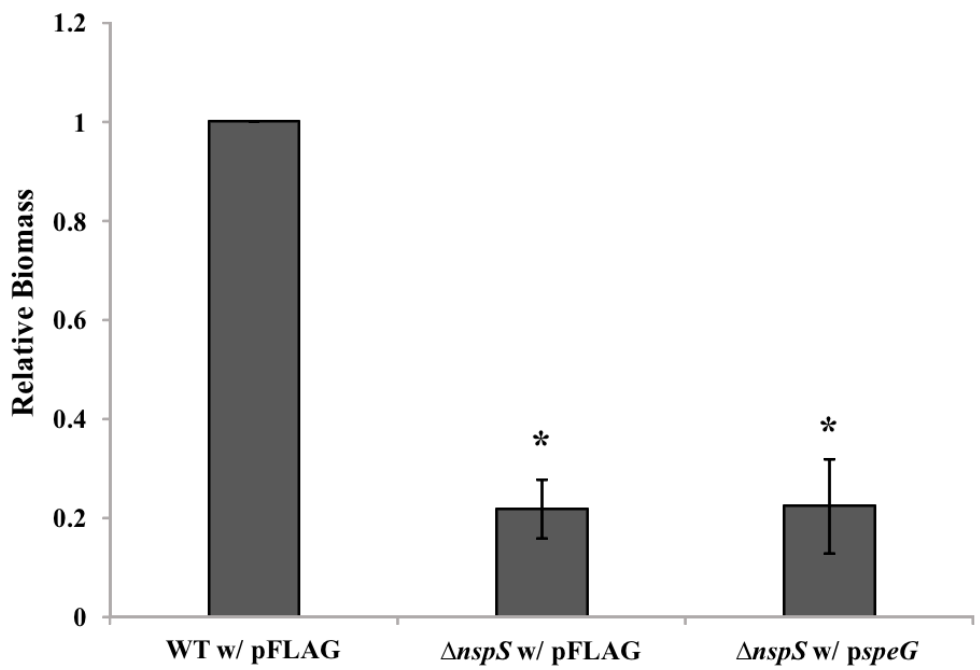


Fig. 31. Biofilm assay of *V. cholerae* $\Delta nspS$ with *pspeG* or pFLAG-CTC. Biofilms were formed in borosilicate tubes in LB broth for 24 hours at 27 °C without ampicillin, and quantified as described in Materials and Methods. Relative biomass was calculated using the following equation OD_{655} mutant/ OD_{655} wild-type (Y-axis). Error bars show standard deviations of eight biological replicates. A star indicates a significant difference between wild type and the mutants. A p-value of <0.05 was considered significant. WT, wild type.

Conditioned media from *speG* overexpression mutant increase biofilm formation in a *NspS/MbaA*-dependent manner

To determine whether the signal causing an increase in biofilm formation in the *V. cholerae* wild type with *pspeG* and *nspC::kan^R* with *pspeG* strains is an internal or external signal, conditioned medium (CM) biofilm assays were utilized. I hypothesized that if the positive signal was present in the culture medium, addition of *pspeG* growth medium would increase biofilm formation in wild-type, *nspC::kan^R*, and $\Delta potD1$ strains but not in a $\Delta nspS$ strain, as the signal is hypothesized to work through the NspS/MbaA signaling complex. Indeed, the addition of *pspeG* conditioned medium to *V. cholerae* wild type, *nspC::kan^R*, and $\Delta potD1$ mutants significantly increased biofilm formation, compared to LB medium and

pFLAG-CTC conditioned medium (Fig. 32). Conversely, *pspeG* conditioned medium did not increase biofilm formation in the *ΔnspS* mutant (Fig. 32).

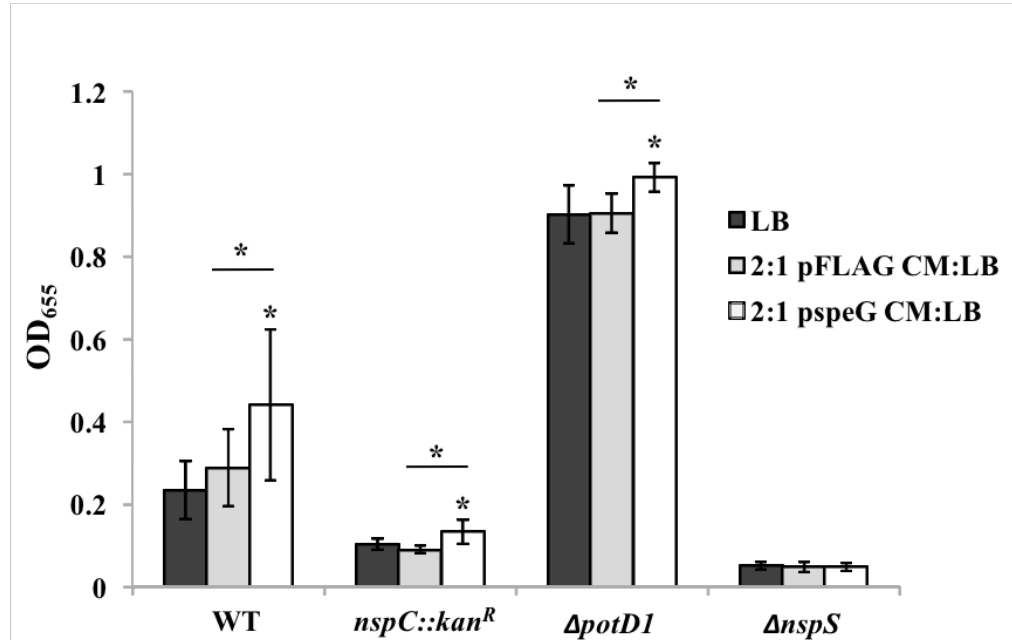


Fig. 32. Effect of *pspeG* or pFLAG-CTC conditioned medium on wild type, *nspC::kan^R*, *ΔpotD1*, and *ΔnspS* biofilm formation. Biofilms were formed in borosilicate tubes in LB broth for 24 hours at 27 °C and quantified as described in Materials and Methods. Error bars show standard deviations of nine biological replicates. A star indicates a significant difference between LB and *pspeG* conditions. An underlined star indicates a significantly significant difference between pFLAG-CTC and *pspeG* conditions. A p-value of <0.05 was considered significant. WT, wild type.

Polyamine concentrations in *pspeG* cellular and media extracts

Considering the addition of *pspeG* conditioned medium significantly enhanced wild type, *nspC::kan^R*, and *ΔpotD1* biofilm formation in a NspS/MbaA-dependent manner, I hypothesized that some metabolite in the *pspeG* medium was responsible for this effect. A standard mix of known polyamines, as well as an *N^δ*-acetylspermidine standard, were benzoylated and analyzed by HPLC to identify possible unknown peaks (Fig. 33).

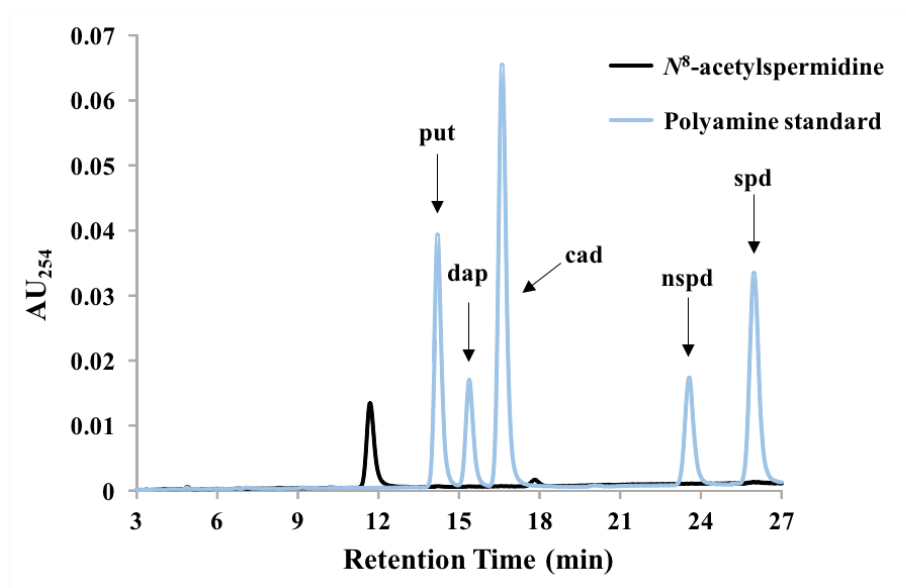


Fig. 33. *N*⁸-acetylspermidine and polyamine standard. A standard mix containing 0.1 mM of each polyamine was benzoylated and analyzed by HPLC. Labeled peaks on the chromatogram correspond to putrescine (put), diaminopropane (dap), cadaverine (cad), norspermidine (nspd), and spermidine (spd). Only 3 to 27 minutes of a 40 minute run are plotted for clarity.

To extract media polyamines, a day culture was diluted from an overnight culture and polyamines were extracted from the media at 0, 2, 4, and 6 hours. The supernatants used for HPLC analyses were separate from those used in conditioned medium biofilm assays. An unknown peak at 4 minutes (represented by “x”) was detected in the *pspeG* media extracts (Fig. 34). Interestingly, this peak doubled in size every two hours (maximum detection at 0.3 AU₂₅₄), and was significantly higher than the known polyamines present in the media (Fig. 34). The pFLAG-CTC media exhibited the same unknown peak around 4 minutes (represented by “x”); (Fig. 35); however, this peak was significantly less (maximum detection at 0.09 AU₂₅₄) than that detected in the *pspeG* media. Considering the wild type with pFLAG-CTC strain still expresses the *speG* gene, it is not surprising that the wild type with pFLAG-CTC media exhibits the same unknown peak as detected in the *pspeG* medium extract, albeit at lower amounts. Based on my hypotheses, I suspected that the unknown peak

in both the *pspeG* and pFLAG-CTC media may be a modified form of norspermidine, such as acetylated norspermidine, or some other polyamine that is enhancing biofilm levels. Of importance and as previously observed [34], no norspermidine was detected in the spent media (Fig. 34, Fig. 35), suggesting that this polyamine is either not being exported out of the cell, or is being exported in a modified form.

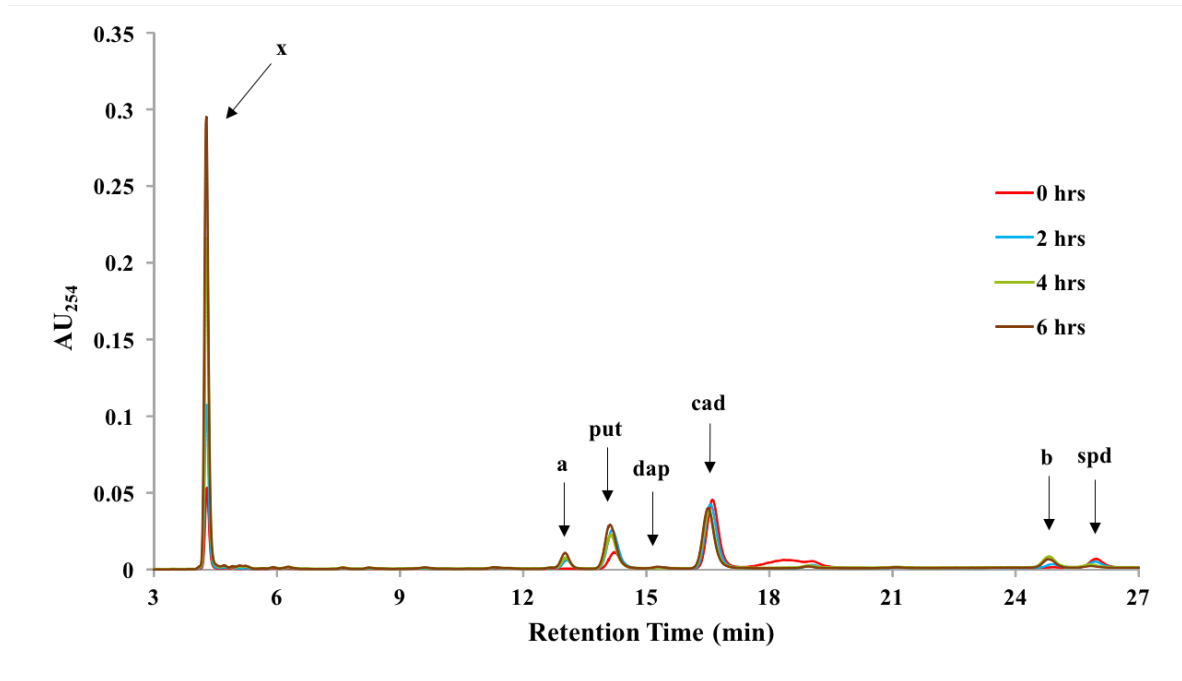


Fig. 34. Polyamine content in *pspeG* culture medium. Polyamines were extracted, benzoylated, and analyzed by HPLC. Labeled peaks on the chromatogram correspond to putrescine (put), diaminopropane (dap), cadaverine (cad), and spermidine (spd). x, a, and b represent unknown peaks. Only 3 to 27 minutes of a 40 minute run are plotted for clarity.

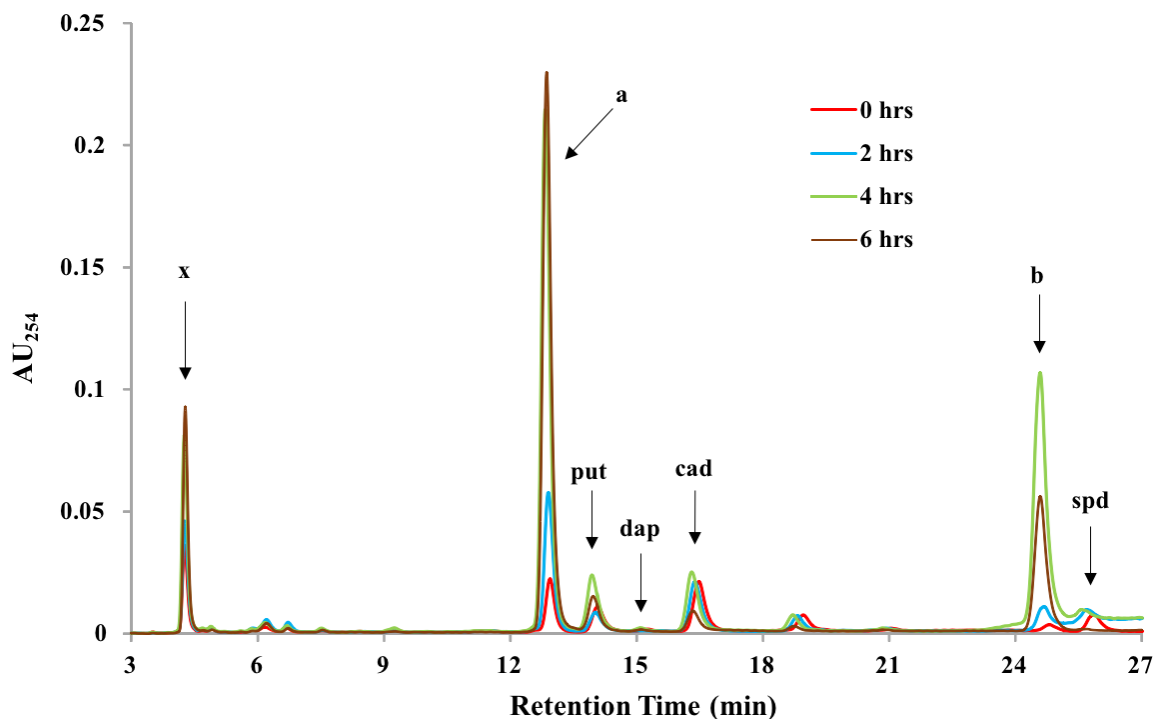


Fig. 35. Polyamine content in pFLAG-CTC culture medium. Polyamines were extracted, benzoylated, and analyzed by HPLC. Labeled peaks on the chromatogram correspond to putrescine (put), diaminopropane (dap), cadaverine (cad), and spermidine (spd). x, a, and b represent unknown peaks. Only 3 to 27 minutes of a 40 minute run are plotted for clarity.

Acetylated norspermidine is not easily attainable for use as an HPLC standard.

Therefore, I next wanted to indirectly determine whether the unknown peak in the *pspeG* medium was in fact a modified form of norspermidine. If it were a modified form of norspermidine, such as acetylated norspermidine, I would not expect to detect this same unknown peak when analyzing *nspC::kan^R* without *pspeG* spent media. Interestingly, when observing the HPLC chromatogram, the same unknown peak at 4 minutes was detected in the media of the *nspC::kan^R* mutant (represented by “x”), albeit at much lower levels (maximum detection at 0.035 AU₂₅₄) than both the *pspeG* and pFLAG-CTC media (Fig. 36). As previously mentioned, a *nspC::kan^R* mutant is unable to synthesize norspermidine, and thus, SpeG would be unable to acetylate this polyamine and transport it out of the cell. These data

suggest that the unknown peak at 4 minutes in the *pspeG* and pFLAG-CTC media is not acetylated norspermidine. However, further metabolite analyses must be conducted to confirm both the identity of the unknown peak and if this is the polyamine, modified or not, responsible for the enhanced biofilm phenotype in wild type, *nspC::kan^R*, and Δ *potD1* mutants.

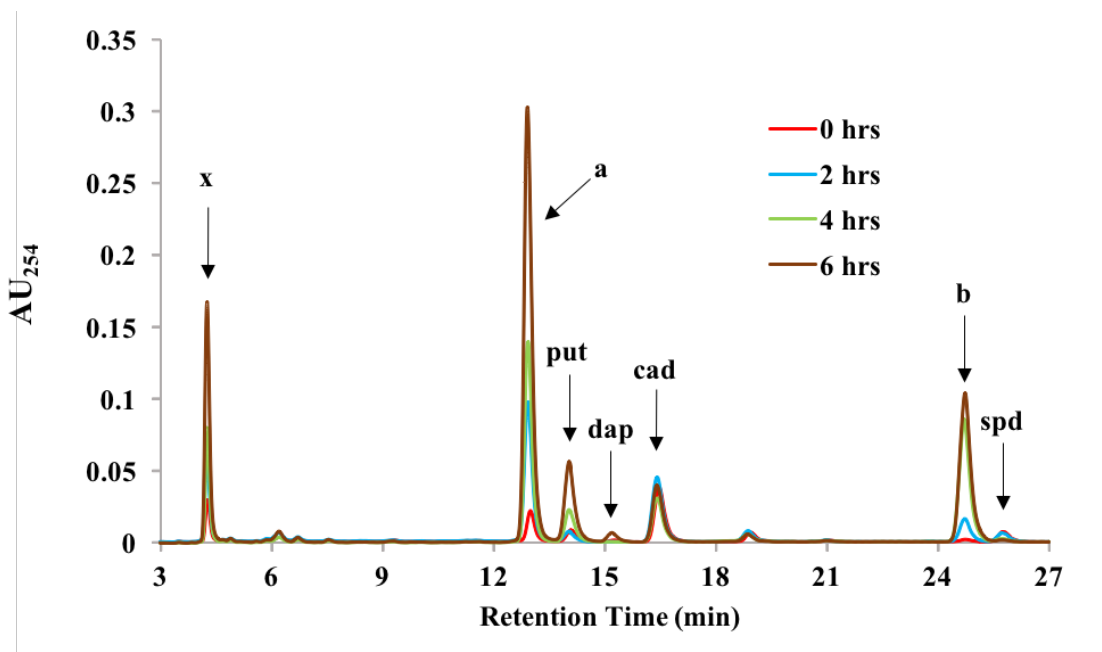


Fig. 36. Polyamine content in *nspC::kan^R*, without *pspeG*, culture medium. Polyamines were extracted, benzoylated, and analyzed by HPLC. Labeled peaks on the chromatogram correspond to putrescine (put), diaminopropane (dap), cadaverine (cad), and spermidine (spd). x, a, and b represent unknown peaks. Only 3 to 27 minutes of a 40 minute run are plotted for clarity.

Additional unknown metabolites eluted before putrescine and spermidine (represented by “a” and “b”, respectively) in the wild type with *pspeG*, wild type with pFLAG-CTC, and *nspC::kan^R* media extracts. These metabolites are consistently found in the wild type with *pspeG*, wild type with pFLAG-CTC, and *nspC::kan^R* media extracts, suggesting that they may be of biological significance. While the identity of these peaks is unknown, it is possible that the peaks represent some metabolites perhaps excreted to

maintain intracellular homeostasis. Of importance, unknown peak “x” is consistently found in *V. cholerae* wild type media; however, unknown peaks “a” and “b” are not (Isenhower and Karatan, unpublished data). For media extractions, the wild type with pFLAG-CTC mutant is grown in the presence of ampicillin. As previously mentioned, the addition of ampicillin led to an overall decrease in wild type with pFLAG-CTC biofilm formation compared to when the strain was grown without ampicillin. Considering the wild type with pFLAG-CTC and *nspC::kan^R* mutants are both low biofilm-formers, it is possible that unknown peaks “a” and “b” represent some type of biofilm-inhibiting metabolite. Although the identity and function of these peaks is unknown, it is intriguing that unknown peak “x” seems to have an inverse relationship with unknown peak “a”. That is, when concentrations of unknown peak “x” are high, concentrations of unknown peak “a” are low, and vice versa.

To see whether a difference in intracellular polyamine content could explain either the significant increase of the unknown peak in the *pspeG* media or the increase in biofilm formation, I next measured cellular polyamine levels. When comparing the cellular polyamine content between these two strains, there was not a significant difference detected (Fig. 37). Interestingly, norspermidine levels did not change between these two strains (Fig. 37), corroborating previous results that this polyamine does not seem to accumulate in the cell [34]. As previously mentioned, polyamine levels are tightly controlled in cells, so it is possible that some type of regulatory function, feedback mechanism, and/or modification process is maintaining polyamine homeostasis.

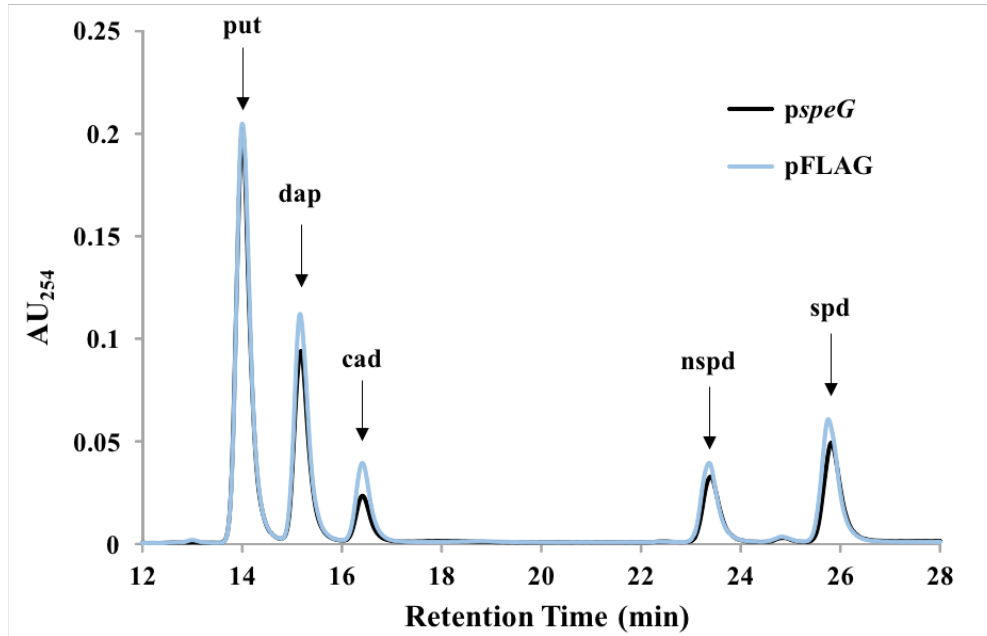


Fig. 37. Cellular polyamine content of wild-type *V. cholerae* with *pspeG* and pFLAG-CTC. Polyamines were extracted, benzoylated, and analyzed by HPLC. Labeled peaks on the chromatogram correspond to putrescine (put), diaminopropane (dap), cadaverine (cad), norspermidine (nspd), and spermidine (spd). Only 12 to 28 minutes of a 40 minute run are plotted for clarity.

Discussion

The purpose of this study was to assess the role of spermidine/spermine-*N*'-acetyltransferase, SpeG, in *V. cholerae* biofilm formation. I hypothesized that SpeG acetylates norspermidine to facilitate its transfer out of the cell in an effort to mitigate intracellular norspermidine toxicity, and that once transported out into the extracellular environment, acetylnorspermidine can bind the periplasmic binding protein NspS, inhibit MbaA phosphodiesterase activity, and ultimately increase levels of c-di-GMP, *vps* gene expression, and biofilm formation (Fig. 38).

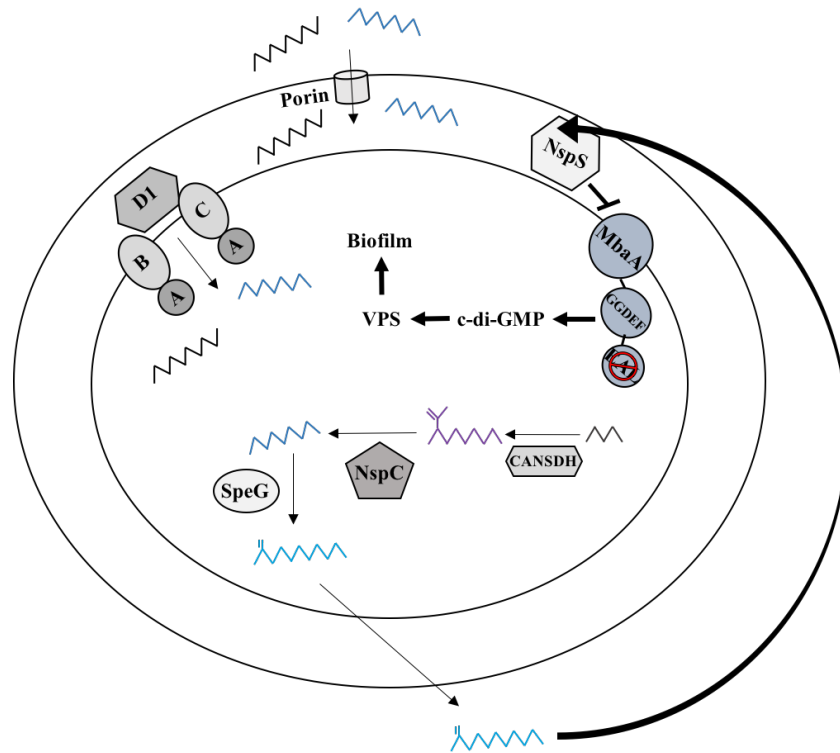


Fig. 38. Hypothetical model of the role of SpeG in *V. cholerae* biofilm formation. NspC synthesizes norspermidine by the decarboxylation of carboxynorspermidine. Intracellular norspermidine can be acetylated by the SpeG enzyme and transported out of the cell, where it can then bind to NspS, inhibit MbaA phosphodiesterase activity, and increase c-di-GMP, *Vibrio* polysaccharide (VPS), and biofilm formation. Diaminopropane is represented by a small black zig-zag, carboxynorspermidine is represented by a purple branched zig-zag, norspermidine is represented by a blue zig-zag, spermidine is represented by a black zig-zag, and acetylnorspermidine is represented by a cyan branched zig-zag. The PotABCD1 transporter is denoted as A, B, C, and D1.

Through this work I have shown that the *speG* gene may be essential for *V. cholerae*, as attempts to delete this gene were unsuccessful. Polyamines are not only required for cell growth and development, but they are also essential regulators of gene transcription and translation, enzymatic activities, and modulation of ion channels [35, 36]. Therefore, intracellular polyamine levels are tightly regulated by import and export mechanisms, as well as by biosynthetic, interconversion, and acetyltransferase enzymes [37]. Without the *speG*

gene, *V. cholerae* may not have a means to avert polyamine toxicity, leading to an accumulation of polyamines at levels toxic to the cells.

Additionally, my data suggest that SpeG is a positive regulator of biofilm formation. Since a *speG* deletion mutant could not be constructed, the *speG* gene was overexpressed from a plasmid in *V. cholerae* wild type, *nspC::kan^R*, *ΔpotD1*, and *ΔnspS* backgrounds and biofilm formation was quantified. I expected one of two possible phenotypes from overexpressing *speG* in wild-type *V. cholerae*. First, it was possible that overexpressing *speG* in wild-type *V. cholerae* would not change biofilm formation, as both polyamine levels and SpeG acetyltransferase activity are tightly regulated to maintain polyamine homeostasis [37, 38]. It was also possible that by overexpressing *speG* in wild-type *V. cholerae*, there would be an increase in the amount of acetylnorspermidine transferred out of the cell, which could bind to NspS, enhance the inhibitory effect of NspS on MbaA, and lead to a significant increase in biofilm formation.

Indeed, I found that overexpressing the *speG* gene significantly increased biofilm formation in wild-type *V. cholerae*. These results were consistent with my hypothesis that SpeG can acetylate norspermidine and facilitating its transfer out of the cell, where it could bind NspS and lead to an increase in biofilm formation. To further delineate the mechanism behind this effect, biofilm formation of *pspeG* in *nspC::kan^R*, *ΔnspS*, and *ΔpotD1* backgrounds was also quantified. The PotABCD1 transporter imports both spermidine and norspermidine, and SpeG has been shown to acetylate both of these polyamines [47] (Misty Kuhn, personal correspondence). While a *ΔpotD1* mutant is incapable of importing spermidine and norspermidine, NspC is still present in this mutant to synthesize norspermidine. Therefore, in a *ΔpotD1* mutant, I hypothesized that norspermidine could still

be acetylated by SpeG and that extracellular acetylnorspermidine could be sensed by NspS and lead to an increase in biofilm formation. However, there was no significant difference in biofilm levels between the *ΔpotD1* with *pspeG* and *ΔpotD1* with pFLAG-CTC mutants. As previously mentioned, biofilm levels in the *ΔpotD1* mutant may already be at a maximum, therefore, the effect of overexpressing *speG* may be difficult to measure. To determine whether the increase in biofilm formation in the wild type with *pspeG* strain was in fact due to acetylated norspermidine being transported out of the cell, I also overexpressed *speG* in a *nspC::kan^R* mutant. Inconsistent with my hypothesis, the presence of *pspeG* also enhanced biofilm formation in the *nspC::kan^R* mutant. This mutant is incapable of synthesizing norspermidine; therefore, under these conditions, it would not be possible for SpeG to acetylate this polyamine and facilitate its transfer out of the cell. These results suggested that while *pspeG* may enhance biofilm formation in wild-type *V. cholerae* through the acetylation of norspermidine, in the absence of the *nspC* gene, *pspeG* acetylates another polyamine that in its modified form is able to bind NspS to enhance biofilm formation. Previous work has found that *V. cholerae* SpeG is able to acetylate the polyamine putrescine when concentrations of both the polyamine and enzyme are high [47]. Alternatively, previous work has found that in a *nspC::kan^R* mutant, intracellular levels of the polyamine diaminopropane significantly increase; however, this effect can be reversed by the addition of norspermidine to the growth medium [32]. Diaminopropane is converted via carboxynorspermidine dehydrogenase to the intermediate carboxynorspermidine, which is further converted to norspermidine by NspC. Therefore, diaminopropane accumulates in the cell when NspC is not present to convert the carboxynorspermidine intermediate to norspermidine. Although diaminopropane is a shorter polyamine, it consists of an aminopropyl group. Of importance,

it has been shown that molecules containing an aminopropyl moiety are more effective substrates for polyamine acetyltransferases [39, 44]. It is clear, however, that the metabolite responsible for enhancing biofilm formation in wild type and the *nspC::kan^R* mutant is acting through NspS, as biofilm levels are unchanged between the $\Delta nspS$ with *pspeG* and $\Delta nspS$ with pFLAG-CTC mutants. These data suggest that this unknown metabolite may bind to NspS, enhance the inhibitory effect of NspS on MbaA, and lead to an increase in biofilm formation.

To elucidate whether this positive signal was acting internally or externally to increase biofilm formation, conditioned medium biofilm assays were utilized. I hypothesized that if the metabolite were exported out of the cell into the culture medium of the wild type with *pspeG* strain, the addition of *pspeG* spent medium would enhance biofilm formation in wild-type, *nspC::kan^R*, and $\Delta potD1$ strains. Furthermore, if the metabolite were acting through the NspS/MbaA signaling system, there would be no effect of adding wild type with *pspeG* spent medium on a $\Delta nspS$ mutant. Indeed, the addition of wild type with *pspeG* conditioned medium to *V. cholerae* wild type, *nspC::kan^R*, and $\Delta potD1$ strains significantly increased biofilm formation compared to LB medium and wild type with pFLAG-CTC medium. These data suggest that the metabolite responsible for the increase in biofilm formation is an external signal. Furthermore, this metabolite does not increase biofilm formation by import through the PotABCD1 transporter as addition of wild type with *pspeG* conditioned medium significantly enhanced biofilm formation in the $\Delta potD1$ mutant. Addition of wild type with *pspeG* conditioned medium did not change biofilm formation of a $\Delta nspS$ mutant, suggesting that this external metabolite is increasing biofilm formation in a NspS/MbaA-dependent manner. Taken together, these data suggest that the positive signal

for biofilm formation is indeed external, as some metabolite, perhaps an acetylated polyamine, in the wild type with *pspeG* spent medium is responsible for the increase in biofilm formation. Furthermore, these data indicate that the positive signal enhancing biofilm formation is acting through the NspS/MbaA signaling complex.

I next wanted to determine if this metabolite could be detected in the spent medium by HPLC. When wild type with *pspeG* media extracts were analyzed, there was an unknown peak detected at 4 minutes. Of importance, this unknown peak doubled in size every two hours and had a maximum detection of 0.3 AU₂₅₄. This unknown peak was significantly higher than all the eluted polyamines. In analyzed pFLAG-CTC spent media, the same unknown peak was detected at 4 minutes; however, this peak was significantly lower than the peak detected in the *pspeG* media. If this unknown peak was in fact the metabolite responsible for the increase in biofilm formation, it would be reasonable to detect it in both the *pspeG* and pFLAG-CTC medium, as the wild type with pFLAG-CTC still expresses the *speG* gene from the chromosome. However, the *pspeG* strain contains many copies of *speG* and would therefore facilitate the export of many more metabolites that could perhaps bind NspS. It is intriguing that this unknown peak was accumulating in the wild type with *pspeG* spent media, a condition that was shown to enhance biofilm formation. It is possible that this unknown peak is representative of the metabolite, and perhaps acetylated polyamine, responsible for enhancing biofilm formation through the NspS/MbaA signaling complex.

Overexpressing *speG* in a *nspC::kan^R* background increased biofilm formation, suggesting that under these conditions, the metabolite responsible for this enhancement is not acetylated norspermidine. To further confirm these results, I next analyzed *nspC::kan^R* spent media to see if the same unknown peak in the wild type with *pspeG* media could be detected.

Indeed, at 4 minutes, the same unknown peak was detected in the *nspC::kan^R* spent media. These results corroborated previous results that the unknown peak is not acetylated norspermidine, as the *nspC::kan^R* mutant is incapable of synthesizing norspermidine. It is important to note that the unknown peak in the *nspC::kan^R* spent media was detected at a much lower concentration than in the wild type with *pspeG* media. The possibility remains that the unknown peak in the wild type with *pspeG* media is in fact acetyl-norspermidine, and that some other metabolite is eluting at the same time in the *nspC::kan^R* spent media extract. It would be interesting to analyze the spent media of a *nspC::kan^R* with *pspeG* mutant to determine if an additional unknown metabolite can be detected, or if there is a difference in the concentration of the unknown metabolite of interest. This may provide insight into the mechanism by which overexpression of *speG* in the *nspC::kan^R* mutant increases biofilm formation. As previously stated, it is also possible that the unknown peak is acetyl-diaminopropane. To test this hypothesis, it would be necessary to block the synthesis of diaminopropane. Diaminopropane is synthesized from L-glutamate and aspartate β -semialdehyde by the intermediate L-2,4,-diaminobutyrate (DABA) by the enzymes DABA aminotransferase (DABA AT) and DABA decarboxylase (DABA DC) [57, 58]. By blocking the synthesis of diaminopropane, it may be possible to indirectly determine if the unknown peak in the wild type with *pspeG* and *nspC::kan^R* spent media extracts is acetyl-diaminopropane. Additionally, a metabolite analysis could be conducted to confirm the identity of the unknown peak, and if it is in fact the metabolite responsible for enhancing biofilm formation. Liquid chromatography-mass spectrometry (LC-MS) could be utilized to identify the unknown peak in the wild type with *pspeG* media. LC-MS fragmentation, as described by Kim *et al* [59], could separate the polyamine components of the wild type with

pspeG media, while providing structural identity of each polyamine component. This method could also be utilized to identify the other unknown peaks, “a” and “b,” in the media extracts. Considering these peaks are consistently found in the media of wild type with *pspeG*, wild type with pFLAG-CTC, and *nspC::kan^R* mutants, they likely do not represent artifacts, but instead, metabolites of some biological significance.

To see whether a difference in intracellular polyamine content could explain either the significant increase of the unknown peak in the wild type with *pspeG* media or the increase in biofilm formation, I next analyzed intracellular polyamine concentrations. There was no difference in polyamine concentrations between the wild type with *pspeG* and wild type with pFLAG-CTC strains. These results suggested that the increase in biofilm formation was not due to an intracellular accumulation of some polyamine, which corroborates the conditioned medium biofilm assay results that the positive signal for biofilm formation is indeed external.

Recently, a novel ABC-type exporter, SapBCDF, was identified in *E. coli*, which mediates export of putrescine from the cytosol to the extracellular environment to regulate intracellular concentrations of this polyamine [60]. Of importance, *V. cholerae* contains the SapBCDF exporter; however, it has yet to be characterized. It is possible that *V. cholerae* may utilize this polyamine exporter to transport norspermidine from the cytosol to the periplasm in order to regulate intracellular levels. Once in the periplasm, it may then act as a signal to regulate biofilm levels through NspS/MbaA. In *Bacillus subtilis*, the spermidine/spermine-*N*-acetyltransferase BltD works in conjunction with Blt, a multidrug export protein responsible for acetylated spermidine export [44]. Therefore, it is possible that SpeG works in conjunction with an exporter, such as SapBCDF, which could also be exporting acetylated

polyamines into the extracellular environment to regulate biofilm formation through NspS/MbaA. Deletions of the *sapBCDF* genes that encode the exporter could be constructed to test this hypothesis. Media extract analyses and biofilm assays could be performed in a strain void of a component of the SapBCDF exporter and with a *speG* overexpression. If the SapBCDF exporter is indeed involved in the export of either polyamines or acetylated polyamines, there may be a difference in biofilm levels, as well as intracellular or extracellular polyamine content.

In conclusion, overexpression of the *speG* gene significantly enhances biofilm formation in *V. cholerae* wild type and *nspC::kan^R* backgrounds in a NspS/MbaA-dependent manner. Furthermore, an external metabolite significantly increased biofilm formation in a NspS/MbaA-dependent manner. Enhancement of biofilm formation by SpeG may be due to the acetylation of norspermidine; however, in the absence of *nspC*, another metabolite in the spent medium may be responsible for this effect. Future work must be completed to understand the mechanism by which SpeG promotes biofilm formation in *V. cholerae*. To identify the metabolite responsible for the increase in biofilm formation by SpeG, metabolomics experiments will need to be conducted.

References

1. Faruque SM, Albert MJ, Mekalanos JJ. Epidemiology, Genetics, and Ecology of Toxigenic *Vibrio cholerae*. *Microbiol Mol Biol Rev.* 1998; 62(4):1301-1314.
2. Costerton JW, Cheng K, Geesey GG, Ladd TI, Nickel JC, Dasgupta M, et al. Bacterial biofilms in nature and disease. *Annu Rev Microbiol.* 1987; 41(1):435-464.
3. Costerton JW, Lewandowski Z, Caldwell DE, Korber DR, Lappin-Scott HM. Microbial biofilms. *Annu Rev Microbiol.* 1995; 49(1):711-745.
4. Donlan RM, Costerton JW. Biofilms: survival mechanisms of clinically relevant microorganisms. *Clin Microbiol Rev.* 2002; 15(2):167-193.
5. Elasri MO, Miller RV. Study of the response of a biofilm bacterial community to UV radiation. *Appl Environ Microbiol.* 1999; 65(5):2025-2031.
6. Prigent-Combaret C, Vidal O, Dorel C, Lejeune P. Abiotic surface sensing and biofilm-dependent regulation of gene expression in *Escherichia coli*. *J Bacteriol.* 1999; 181(19):5993-6002.
7. McNeill K, Hamilton I. Acid tolerance response of biofilm cells of *Streptococcus mutans*. *FEMS Microbiol Lett.* 2003; 221(1):25-30.
8. Cash RA, Music SI, Libonati JP, Snyder MJ, Wenzel RP, Hornick RB. Response of man to infection with *Vibrio cholerae*. I. Clinical, serologic, and bacteriologic responses to a known inoculum. *J Infect Dis.* 1974; 129(1):45-52.

9. Hall-Stoodley L, Stoodley P. Biofilm formation and dispersal and the transmission of human pathogens. *Trends Microbiol.* 2005; 13(1):7-10.
10. Hornick R, Music S, Wenzel R, Cash R, Libonati J, Snyder M, et al. The Broad Street pump revisited: Response of volunteers to ingested cholera vibrios. *Bull N Y Acad Med.* 1971; 47(10):1181.
11. Heithoff DM, Mahan MJ. *Vibrio cholerae* biofilms: Stuck between a rock and a hard place. *J Bacteriol.* 2004; 186(15):4835-4837.
12. Krasteva PV, Fong JC, Shikuma NJ, Beyhan S, Navarro MV, Yildiz FH, et al. *Vibrio cholerae* VpsT regulates matrix production and motility by directly sensing cyclic di-GMP. *science.* 2010; 327(5967):866-868.
13. Karatan E, Watnick P. Signals, regulatory networks, and materials that build and break bacterial biofilms. *Microbiol Mol Biol Rev.* 2009; 73(2):310-347.
14. Beyhan S, Bilecen K, Salama SR, Casper-Lindley C, Yildiz FH. Regulation of rugosity and biofilm formation in *Vibrio cholerae*: Comparison of VpsT and VpsR regulons and epistasis analysis of vpsT, vpsR, and hapR. *J Bacteriol.* 2007; 189(2):388-402.
15. Sutherland IW. The biofilm matrix—an immobilized but dynamic microbial environment. *Trends Microbiol.* 2001; 9(5):222-227.
16. Silva AJ, Benitez JA. *Vibrio cholerae* Biofilms and Cholera Pathogenesis. *PLoS Negl Trop Dis.* 2016; 10(2):e0004330.
17. Kaper JB, Morris JG, Jr., Levine MM. Cholera. *Clin Microbiol Rev.* 1995; 8(1):48-86.

18. Stanley NR, Lazazzera BA. Environmental signals and regulatory pathways that influence biofilm formation. *Mol Microbiol.* 2004; 52(4):917-924.
19. Karatan E, Duncan TR, Watnick PI. NspS, a predicted polyamine sensor, mediates activation of *Vibrio cholerae* biofilm formation by norspermidine. *J Bacteriol.* 2005; 187(21):7434-7443.
20. Tabor CW, Tabor H. Polyamines. *Ann Rev Biochem.* 1984; 53(1):749-790.
21. Michael AJ. Polyamines in Eukaryotes, Bacteria and Archaea. *J Biol Chem.* 2016; 291(29):14896-14903.
22. Hamana K, Matsuzaki S. Widespread occurrence of norspermidine and norspermine in eukaryotic algae. *J Biochem.* 1982; 91(4):1321-1328.
23. Hamana K, Niitsu M, Samejima K. Unusual polyamines in aquatic plants: The occurrence of homospermidine, norspermidine, thermospermine, norspermine, aminopropylhomospermidine, bis (aminopropyl) ethanediamine, and methylspermidine. *Can J Bot.* 1998; 76(1):130-133.
24. Zappia V, Porta R, Carteni-Farina M, De Rosa M, Gambacorta A. Polyamine distribution in eukaryotes: Occurrence of sym-nor-spermidine and sym-nor-spermine in arthropods. *FEBS Lett.* 1978; 94(1):161-165.
25. Hamana K, Furuchi T, Nakamura T, Hayashi H, Niitsu M. Occurrence of penta-amines, hexa-amines and N-methylated polyamines in unicellular eukaryotic organisms belonging to the phyla Heterokontophyta and Labyrinthulomycota of the subdomain Stramenopiles. *J Gen Appl Microbiol.* 2016:2016.2005. 2001.

26. Lee J, Sperandio V, Frantz DE, Longgood J, Camilli A, Phillips MA, et al. An alternative polyamine biosynthetic pathway is widespread in bacteria and essential for biofilm formation in *Vibrio cholerae*. *J Biol Chem*. 2009; 284(15):9899-9907.
27. McGinnis MW, Parker ZM, Walter NE, Rutkovsky AC, Cartaya-Marin C, Karatan E. Spermidine regulates *Vibrio cholerae* biofilm formation via transport and signaling pathways. *FEMS Microbiol Lett*. 2009; 299(2):166-174.
28. Hanfrey CC, Pearson BM, Hazeldine S, Lee J, Gaskin DJ, Woster PM, et al. Alternative spermidine biosynthetic route is critical for growth of *Campylobacter jejuni* and is the dominant polyamine pathway in human gut microbiota. *J Biol Chem*. 2011; 286(50):43301-43312.
29. Ali MA, Poortvliet E, StrÅkmborg R, Yngve A. Polyamines in foods: Development of a food database. *Adv Food Nutr Res*. 2011; 55.
30. Sanders BE. Characterization of the norspermidine/spermidine ABC-type transporter, PotABCD1, in *Vibrio cholerae*. [M.Sc. Thesis]: Appalachian State University; 2015.
31. Davidson AL, Dassa E, Orelle C, Chen J. Structure, function, and evolution of bacterial ATP-binding cassette systems. *Microbiol Mol Biol Rev*. 2008; 72(2):317-364.
32. Cockerell SR, Rutkovsky AC, Zayner JP, Cooper RE, Porter LR, Pendergraft SS, et al. *Vibrio cholerae* NspS, a homologue of ABC-type periplasmic solute binding proteins, facilitates transduction of polyamine signals independent of their transport. *Microbiol Res*. 2014; 160(5):832-843.

33. Bomchil N, Watnick P, Kolter R. Identification and characterization of a *Vibrio cholerae* gene, *mbaA*, involved in maintenance of biofilm architecture. *J Bacteriol.* 2003; 185(4):1384-1390.
34. Parker ZM, Pendergraft SS, Sobieraj J, McGinnis MM, Karatan E. Elevated levels of the norspermidine synthesis enzyme NspC enhance *Vibrio cholerae* biofilm formation without affecting intracellular norspermidine concentrations. *FEMS Microbiol Lett.* 2012; 329(1):18-27.
35. Igarashi K, Kashiwagi K. Modulation of cellular function by polyamines. *Int J Biochem Cell Biol.* 2010; 42(1):39-51.
36. Cohen SS. *Guide to the Polyamines.* Oxford, UK: Oxford University Press; 1998.
37. Casero R, Pegg A. Spermidine/spermine N1-acetyltransferase--the turning point in polyamine metabolism. *FASEB J.* 1993; 7(8):653-661.
38. Filippova EV, Kuhn ML, Osipiuk J, Kiryukhina O, Joachimiak A, Ballicora MA, et al. A novel polyamine allosteric site of SpeG from *Vibrio cholerae* is revealed by its dodecameric structure. *J Molec Biol.* 2015; 427(6):1316-1334.
39. Forouhar F, Lee I-S, Vujcic J, Vujcic S, Shen J, Vorobiev SM, et al. Structural and functional evidence for *Bacillus subtilis* PaiA as a novel N1-spermidine/spermine acetyltransferase. *J Biol Chem.* 2005; 280(48):40328-40336.
40. Zhang Y, Zhou J, Chang M, Bai L, Shan J, Yao C, et al. Characterization of and functional evidence for Ste27 of *Streptomyces* sp. 139 as a novel spermine/spermidine acetyltransferase. *Biochem J.* 2012; 443(3):727-734.

41. Matsui I, Kamei M, Otani S, Morisawa S, Pegg AE. Occurrence and induction of spermidine-N 1-acetyltransferase in *Escherichia coli*. *Biochem Biophys Res Commun*. 1982; 106(4):1155-1160.
42. Fukuchi J-i, Kashiwagi K, Takio K, Igarashi K. Properties and structure of spermidine acetyltransferase in *Escherichia coli*. *J Biol Chem*. 1994; 269(36):22581-22585.
43. Bai L, Chang M, Shan J, Jiang R, Zhang Y, Zhang R, et al. Identification and characterization of a novel spermidine/spermine acetyltransferase encoded by gene ste26 from *Streptomyces* sp. 139. *Biochim*. 2011; 93(9):1401-1407.
44. Woolridge DP, Martinez JD, Stringer DE, Gerner EW. Characterization of a novel spermidine/spermine acetyltransferase, BltD, from *Bacillus subtilis*. *Biochem J*. 1999; 340(3):753-758.
45. Martini C, Michaux C, Bugli F, Arcovito A, Iavarone F, Cacaci M, et al. The polyamine N-acetyltransferase-like enzyme PmvE plays a role in the virulence of *Enterococcus faecalis*. *Infect Immun*. 2015; 83(1):364-371.
46. Joshi GS, Spontak JS, Klapper DG, Richardson AR. Arginine catabolic mobile element encoded speG abrogates the unique hypersensitivity of *Staphylococcus aureus* to exogenous polyamines. *Mol Microbiol*. 2011; 82(1):9-20.
47. Kuhn ML, Majorek KA, Minor W, Anderson WF. Broad-substrate screen as a tool to identify substrates for bacterial Gcn5-related N-acetyltransferases with unknown substrate specificity. *Protein Sci*. 2013; 22(2):222-230.
48. Pegg AE. Spermidine/spermine-N1-acetyltransferase: a key metabolic regulator. *Am J Physiol Endocrinol Metab*. 2008; 294(6):E995-E1010.

49. Yamamoto S, Nakao H, Koumoto Y, Shinoda S. Identification of N1-acetylnorspermidine in *Vibrio parahaemolyticus* and an enzyme activity responsible for its formation. *FEMS Microbiol Lett.* 1989; 61(1-2):225-229.
50. Hanahan D. Studies on transformation of *Escherichia coli* with plasmids. *J Molec Biol.* 1983; 166(4):557-580.
51. Miller VL, Mekalanos JJ. A novel suicide vector and its use in construction of insertion mutations: osmoregulation of outer membrane proteins and virulence determinants in *Vibrio cholerae* requires *toxR*. *J Bacteriol.* 1988; 170(6):2575-2583.
52. Waldor MK, Mekalanos JJ. Emergence of a new cholera pandemic: molecular analysis of virulence determinants in *Vibrio cholerae* 0139 and development of a live vaccine prototype. *J Infect Dis.* 1994; 170(2):278-283.
53. Haugo AJ, Watnick PI. *Vibrio cholerae* CytR is a repressor of biofilm development. *Mol Microbiol.* 2002; 45(2):471-483.
54. Metcalf WW, Jiang W, Daniels LL, Kim S-K, Haldimann A, Wanner BL. Conditionally Replicative and Conjugative Plasmids Carrying *lacZ α* for Cloning, Mutagenesis, and Allele Replacement in Bacteria. *Plasmid.* 1996; 35(1):1-13.
55. Morgan DM. *Polyamine protocols*: Springer Science & Business Media; 1998.
56. Dosler S, Karaaslan E. Inhibition and destruction of *Pseudomonas aeruginosa* biofilms by antibiotics and antimicrobial peptides. *Peptides.* 2014; 62:32-37.
57. Ikai H, Yamamoto S. Identification and analysis of a gene encoding L-2, 4-diaminobutyrate: 2-ketoglutarate 4-aminotransferase involved in the 1, 3-diaminopropane production pathway in *Acinetobacter baumannii*. *J Bacteriol.* 1997; 179(16):5118-5125.

58. Ikai H, Yamamoto S. Cloning and expression in *Escherichia coli* of the gene encoding a novel L-2, 4-diaminobutyrate decarboxylase of *Acinetobacter baumannii*. *FEMS Microbiol Lett.* 1994; 124(2):225-228.
59. Kim SH, Wang Y, Khomutov M, Khomutov A, Fuqua C, Michael AJ. The essential role of spermidine in growth of *Agrobacterium tumefaciens* is determined by the 1, 3-diaminopropane moiety. *ACS Chem Biol.* 2016; 11(2):491.
60. Sugiyama Y, Nakamura A, Matsumoto M, Kanbe A, Sakanaka M, Higashi K, et al. A novel putrescine exporter SapBCDF of *Escherichia coli*. *J Biol Chem.* 2016; 291(51):26343-26351.

Vita

Caitlin Wotanis was born in Princeton, New Jersey and attended Providence High School in Charlotte, North Carolina. After graduating high school, she went to Appalachian State University in Boone, NC and graduated in 2012 with a Bachelor of Arts in Biology and a minor in Chemistry. She then spent two years teaching high school health in Rome, Italy, after which she began working in Dr. Ece Karatan's lab in 2015. Having received her Master of Science in Cell and Molecular Biology from Appalachian State in August 2017, she is pursuing a career in biological research.